THE ASTROPHYSICAL JOURNAL, 264:485–507, 1983 January 15

MAGNETOHYDRODYNAMIC SHOCK WAVES IN MOLECULAR CLOUDS

B. T. DRAINE,[1] W. G. ROBERGE,[1,2] AND A. DALGARNO[2]
Received 1981 November 6; accepted 1982 July 6

ABSTRACT

The structure of shock waves in molecular clouds is calculated, including the effects of ion-neutral streaming driven by the magnetic field. It is found that shock waves in molecular clouds will usually be *C*-type shock waves, mediated entirely by the dissipation accompanying ion-neutral streaming, and in which all of the hydrodynamic variables are continuous. Detailed results are presented for magnetohydrodynamic shock waves propagating at speeds in the range of 5–50 km s^{-1} in molecular clouds with preshock densities $n_H = 10^2$, 10^4, and 10^6 cm^{-3}. Graphs are constructed of the effective "excitation temperatures" of the rotational and vibrational levels of H_2 in the shocked gas. The effects of chemical changes in the composition of oxygen-bearing molecules are investigated, and the contributions to the cooling of the shocked gas by emission from H_2, CO, OH, and H_2O are evaluated. Predictions are made of the intensities of the rotation-vibration lines of H_2 and of the fine-structure lines of O I and C I. Magnetic fields may lead to a substantial increase in the limiting shock velocity above which dissociation of H_2 takes place: for a cloud of density $n_H = 10^6$ cm^{-3}, the limiting shock speed is ~ 45 km s^{-1}. The fractional ionization is a critical parameter affecting the shock structure, and the processes acting to change the ionization in the shock are examined. Magnetic field effects enhance the sputtering of grain mantles in dense gas: H_2O ice mantles can be substantially eroded in $v_s \geqslant 25$ km s^{-1} shock waves. Grain erosion may contribute to the enhancement of some molecular species in the shocked gas.

Subject headings: hydrodynamics — interstellar: molecules — molecular processes — shock waves

I. INTRODUCTION

In an extended region of active star formation in the Orion molecular cloud OMC-1 containing the Kleinmann-Low nebula and the Becklin-Neugebauer object, molecular gas is observed moving with velocities spanning a range of ~ 100 km s^{-1} (cf. Zuckerman, Kuiper, and Rodriguez Kuiper 1976; Kwan and Scoville 1976; Kuiper, Rodriguez Kuiper, and Zuckerman 1978; Solomon, Huguenin, and Scoville 1981; Genzel *et al.* 1981; Knapp *et al.* 1981). In the same region, vibrationally and rotationally excited molecular hydrogen (Gautier *et al.* 1976; Beckwith *et al.* 1978; Beck, Lacy, and Geballe 1979; Nadeau and Geballe 1979; Ogden *et al.* 1979; Simon *et al.* 1979; Knacke and Young 1980, 1981; Scoville *et al.* 1982; Beck *et al.* 1982; Davis, Larson, and Smith 1982) and rotationally excited CO (Watson *et al.* 1980; Storey *et al.* 1981; Goldsmith *et al.* 1981; van Vliet *et al.* 1981; Stacey *et al.* 1982), HC_3N (Loren *et al.* 1981) and CH_3CN (Loren, Mundy, and Erickson 1981) have been detected. Hypersonic motion in molecular clouds, of which the activity in OMC-1 is a spectacular example, is apparently a common phenomenon (e.g., Zuckerman, Kuiper, and Rodriguez Kuiper 1976; Snell, Loren and Plambeck 1980; Lada and Harvey 1981; Bally 1982; Frerking and Langer 1982; Rodriguez *et al.* 1982; Bally and Lada 1982).

Since the motion is hypersonic, it is tempting to attribute the molecular emission lines and gas acceleration to a shock wave propagating into the quiescent cloud. Previous theoretical shock models ignored the role of magnetic fields in mediating the shock. These models (Kwan 1977; London, McCray, and Chu 1977; Hollenbach and Shull 1977) predicted that the molecular hydrogen would be dissociated if the shock speed exceeded about 25 km s^{-1} (Hollenbach and McKee 1980), yet molecular hydrogen in OMC-1 is observed at velocities of ± 50 km s^{-1} or more. If the fractional ionization in the gas is low, magnetic fields may alter substantially the structure of shock waves (Mullan 1971; Draine 1980) and in particular may lead to much lower levels of excitation and dissociation in the shocked gas than in nonmagnetic shock waves.

We investigate in this paper the structure of shock waves in molecular clouds and give special attention to the mediating influence of magnetic fields, and to the excitation, emissivity, and dissociation of molecular hydrogen. We

[1]Institute for Advanced Study.
[2]Harvard-Smithsonian Center for Astrophysics.

briefly review the theory of magnetohydrodynamic shock waves, and list the important momentum and energy transfer processes. The fractional ionization is a critical parameter, and we investigate in detail the processes which may increase the ionization in the shocked gas. Because O, OH, and H_2O are sources of energy loss in the shocked gas, our calculations include an abbreviated chemistry of oxygen-bearing species. We also estimate the extent to which "icy" grain mantles may be eroded by sputtering.

II. MAGNETOHYDRODYNAMICS

Consider a plane-parallel steady shock wave advancing with velocity v_s into a uniform quiescent medium with a preshock density $n_H = n(H) + 2n(H_2)$ and a magnetic field $\boldsymbol{B}_0$ transverse to v_s. The gas consists of atomic hydrogen, molecular hydrogen, helium with a density $n_{He} = 0.1 n_H$, electrons, and a representative positive ion I^+ with $n(I^+) = n_e$. The generic ion I^+, with an assumed mass $\mu_i = 30 m_H$, is representative of the heavy ion component of dense molecular clouds (cf. de Jong, Dalgarno, and Boland 1980; Prasad and Huntress 1980). The neutral species have a total mass density ρ_n, a mean molecular weight μ_n, a common temperature T_n, and a common flow speed v_n measured in a frame in which the shock is stationary. The ions and electrons have a total mass density ρ_i and flow together with a speed v_i; T_i and T_e are their respective kinetic temperatures. The electrical conductivity of the ions and electrons is assumed to be sufficient so that the electric field effectively vanishes in the local center-of-mass frame of the ions and electrons; with this "magnetohydrodynamic" assumption, the magnetic field varies as $B = B_0 v_s / v_i$.

Formulated in the frame of reference in which the shock is stationary, and neglecting thermal conduction, the conservation laws may be written (Mullan 1971; Draine 1980):

$$\frac{d}{dz}[\rho_n v_n] = S_n, \tag{1}$$

$$\frac{d}{dz}[\rho_i v_i] = -S_n, \tag{2}$$

$$\frac{d}{dz}\left[\rho_n v_n^2 + \rho_n \frac{kT_n}{\mu_n}\right] = F_n, \tag{3}$$

$$\frac{d}{dz}\left[\rho_i v_i^2 + \rho_i \frac{k(T_i + T_e)}{\mu_i} + \frac{B_0^2 v_s^2}{8\pi v_i^2}\right] = F_i, \tag{4}$$

$$\frac{d}{dz}\left[\frac{1}{2}\rho_n v_n^3 + \frac{\rho_n v_n}{\mu_n}\left(\frac{5}{2}kT_n + u_n\right)\right] = G_n + F_n v_n - \frac{1}{2} S_n v_n^2, \tag{5}$$

$$\frac{d}{dz}\left[\frac{1}{2}\rho_i v_i^3 + \frac{5}{2}\rho_i v_i \frac{k(T_i + T_e)}{\mu_i} + \frac{v_s^2 B_0^2}{4\pi v_i}\right] = G_i + G_e + F_i v_i + \frac{1}{2} S_n v_i^2, \tag{6}$$

$$\frac{d}{dz}\left[\frac{3}{2}\rho_i v_i \frac{k(T_i - T_e)}{\mu_i}\right] + \rho_i \frac{k(T_i - T_e)}{\mu_i}\frac{dv_i}{dz} = G_i - G_e, \tag{7}$$

$$\frac{d}{dz}\left[\frac{\rho_n v_n}{\mu_n}\right] = N_n, \tag{8}$$

$$\frac{d}{dz}\left[\frac{\rho_i v_i}{\mu_i}\right] = N_i. \tag{9}$$

S_n is the net rate, per volume, at which ion-electron mass is converted to neutral mass; F_n and F_i are the rates, per volume, at which momentum is added to the neutral and ion fluids, respectively; G_n, G_i, and G_e are the rates, per volume, at which thermal energy is added to the neutral, ion, and electron fluids, respectively, as a result of interactions between the different fluids, interaction with cosmic rays, or emission or absorption of photons; u_n is the internal thermal energy (due to rotation or vibration) per neutral particle; N_n and N_i are the rates, per volume, at which the number of neutrals and ions, respectively, changes as a result of dissociation, ionization, or recombination.

The present study has assumed $F_n = -F_i$, which is equivalent to neglecting the inertia of the dust grains.

For magnetic fields $B_0 > B_{\rm min}$, where

$$B_{\rm min}^2 = 4\pi\left[\rho_i v_s^2 - \frac{5}{3} n_e k(T_i + T_e)\right], \tag{10}$$

an MHD (magnetohydrodynamic) shock wave has a "magnetic precursor," and the ion-electron flow variables ρ_i, v_i, T_i, and T_e are continuous through the shock. MHD shock waves with magnetic precursors may be divided into two classes (Draine 1980): "*J*-type" shocks, in which the neutral flow variables undergo a discontinuous change at a "jump front," and "*C*-type" shocks, in which the neutral flow variables, like the ion-electron flow variables, are continuous functions of position. There is a critical value $B_{\rm crit}$ of the preshock magnetic field such that shocks with $B_{\rm min} < B_0 < B_{\rm crit}$ are *J*-type shocks with magnetic precursors, and shocks with $B_0 > B_{\rm crit}$ are *C*-type. The magnitude of $B_{\rm crit}$ depends not only on the shock speed, preshock density, and ionization, but also on the cooling processes operative in the shock. We shall demonstrate that for shocks with $v_s \lesssim 50$ km s^{-1} propagating in dense molecular clouds, $B_{\rm crit}$ is generally less than the probable field strengths in these regions, and we restrict the present study to *C*-type shock waves.

III. MOMENTUM TRANSFER PROCESSES

Momentum exchange between the neutral and charged fluids occurs both through ion-neutral scattering and by collisions of neutral atoms and molecules with charged dust grains. We ignore distinctions in the elastic scattering cross sections of H, H_2, and He. Momentum transfer due to ion-neutral collisions has been taken to be

$$(F_n)_{IN} = \frac{\mu_n \mu_i}{(\mu_n + \mu_i)} n_e n_n \langle \sigma v \rangle_{IN} (v_i - v_n), \tag{11}$$

where $n_n \equiv n(H_2) + n(H) + n(He)$, and the momentum transfer rate coefficient is taken to be

$$\langle \sigma v \rangle_{IN} \approx \max\left[1.9\times 10^{-9}\ {\rm cm^3\ s^{-1}},\ 1.0\times 10^{-15}{\rm cm^2}|v_n - v_i|\right]. \tag{12}$$

The electron-neutral momentum transfer rate is

$$(F_n)_{eN} = \frac{\mu_n m_e}{(\mu_n + m_e)} n_e n_n \langle \sigma v \rangle_{eN} (v_i - v_n), \tag{13}$$

where (cf. Phelps 1979)

$$\langle \sigma v \rangle_{eN} \approx 1.0\times 10^{-15}\ {\rm cm^2}\left[(v_n - v_i)^2 + \frac{128 k T_e}{9\pi m_e}\right]^{1/2}. \tag{14}$$

Momentum transfer due to collisions between neutral particles and charged dust grains has been computed using equations (37)–(40) of Draine (1980), with an assumed grain potential $-4kT_e/e$.

IV. HEATING AND COOLING PROCESSES

The momentum transfer processes described above are accompanied by energy dissipation. The heating rates corresponding to ion-neutral and electron-neutral scattering are, respectively,

$$(G_n)_{IN} = \frac{\mu_n \mu_i}{(\mu_n + \mu_i)^2} n_e n_n \langle \sigma v \rangle_{IN}\left[\mu_i (v_i - v_n)^2 + 3k(T_i - T_n)\right], \tag{15}$$

$$(G_i)_{IN} = \frac{\mu_n \mu_i}{(\mu_n + \mu_i)^2} n_e n_n \langle \sigma v \rangle_{IN}\left[\mu_n (v_i - v_n)^2 + 3k(T_n - T_i)\right], \tag{16}$$

$$(G_n)_{eN} = \frac{\mu_n m_e}{(\mu_n + m_e)^2} n_e n_n \langle \sigma v \rangle_{eN}\left[m_e (v_i - v_n)^2 + 4k(T_e - T_n)\right], \tag{17}$$

$$(G_e)_{eN} = \frac{\mu_n m_e}{(\mu_n + m_e)^2} n_e n_n \langle \sigma v \rangle_{eN}\left[\mu_n (v_i - v_n)^2 + 4k(T_n - T_e)\right]. \tag{18}$$

The heating rate due to scattering of the neutrals by charged dust grains is given by equations (40), (42), (43) from Draine (1980), with an accomodation coefficient $\alpha = 0.5$; the assumed grain temperature is that listed in Table 3. Heat exchange between electrons and ions occurs by normal Coulomb scattering (Draine 1980).

Energy is deposited in the gas by cosmic ray ionization. Each primary ionization is, on average, associated with 2.78 dissociations of H_2, and provides 4.8 eV of kinetic energy to the dissociation products, and 2.4 eV of kinetic energy to the electron gas:

$$(G_n)_{\rm cr} = 8.46\times10^{-12}\zeta n_{\rm H}\ {\rm ergs}, \tag{19}$$

$$(G_e)_{\rm cr} = 4.23\times10^{-12}\zeta n_{\rm H}\ {\rm ergs}, \tag{20}$$

where ζ is the cosmic ray primary ionization rate for an H atom (Cravens and Dalgarno 1978). Heating also occurs due to H_2 formation from H^- and on dust grains, and we include their contributions (Hollenbach and McKee 1979) in our estimate of the neutral heating rate G_n. We neglected the chemical heating associated with dissociative recombination of H_3^+. Since we are interested only in shock waves in which the temperature rises well above the preshock temperature, the shock structure and emission are insensitive to the actual temperature of the preshock gas; hence it has not been necessary to model in detail the preshock steady state.

Cooling due to collisional excitation of H_2, CO, H_2O, and OH is discussed in § VI below. The neutral gas also loses energy by collisional excitation of the [C I] 609 μm, 370 μm and [O I] 63 μm, 146 μm fine-structure lines. The rate coefficients of Launay and Roueff (1977) for de-excitation by H atoms are approximated by

$$\langle\sigma v\rangle\left({\rm C\ I}\ ^3P_1 \rightarrow {}^3P_0\right) = \left(15+6T_{n3}^{1/2}\right)\times10^{-11}\ {\rm cm^3\ s^{-1}}, \tag{21a}$$

$$\langle\sigma v\rangle\left({\rm C\ I}\ ^3P_2 \rightarrow {}^3P_1\right) = \left(20+30T_{n3}^{1/2}\right)\times10^{-11}\ {\rm cm^3\ s^{-1}}, \tag{21b}$$

$$\langle\sigma v\rangle\left({\rm C\ I}\ ^3P_2 \rightarrow {}^3P_0\right) = \left(9+8T_{n3}^{1/2}\right)\times10^{-11}\ {\rm cm^3\ s^{-1}}, \tag{21c}$$

$$\langle\sigma v\rangle\left({\rm O\ I}\ ^3P_1 \rightarrow {}^3P_2\right) = 3\times10^{-10}T_{n3}^{1/2}\ {\rm cm^3\ s^{-1}}, \tag{22a}$$

$$\langle\sigma v\rangle\left({\rm O\ I}\ ^3P_0 \rightarrow {}^3P_1\right) = 2\times10^{-10}T_{n3}^{1/2}\ {\rm cm^3\ s^{-1}}, \tag{22b}$$

$$\langle\sigma v\rangle\left({\rm O\ I}\ ^3P_0 \rightarrow {}^3P_2\right) = 3.5\times10^{-10}T_{n3}^{1/2}\ {\rm cm^3\ s^{-1}}, \tag{22c}$$

where $T_{n3} \equiv (T_n/10^3\ {\rm K})$. Cross sections for excitation by collisions with H_2 are unavailable; we have assumed rate coefficients for H_2 equal to 50% of those for H. Collisional excitation rate coefficients are obtained from (21) and (22) by detailed balancing. The steady-state populations for the C I and O I fine structure levels have been found assuming three-level atoms subject to collisional excitation and de-excitation by H and H_2, and spontaneous radiative de-excitation (with all lines assumed to be optically thin, and A-values from Nussbaumer and Rusca 1979 for C I, and from Wiese, Smith, and Glennon 1966 for O I).

If T_e rises sufficiently in the shock, electron impact excitation of [C I] $\lambda\lambda$9852 and [O I] $\lambda\lambda$6300,6363 may occur, with cooling rates (Péquignot and Aldrovandi 1976)

$$(G_e)_{\rm C\ I} = -2.3\times10^{-22}\frac{T_e^{1/2}\exp\left(-14667/T_e\right)}{1+7\times10^{-7}n_eT_e^{1/2}}n({\rm C\ I})n_e\ {\rm ergs\ cm^3\ s^{-1}}, \tag{23}$$

$$(G_e)_{\rm O\ I} = -8.2\times10^{-23}\frac{T_e^{1/2}\exp\left(-22840/T_e\right)}{1+7\times10^{-9}n_eT_e^{1/2}}n({\rm O\ I})n_e\ {\rm ergs\ cm^3\ s^{-1}}. \tag{24}$$

Electron impact excitation of electronically excited levels of H and H_2, which may also contribute to the cooling, was included in our calculations using the cross section data of Srivastava and Jensen (1977), Blevin, Fletcher, and Hunter (1978), Chung and Lin (1978), Fliflet and McKoy (1980), and Weatherland (1980). They prove to be important only in shocks in which the electron temperature exceeds 10^4 K.

V. IONIZATION PROCESSES

The structure of MHD shock waves depends crucially on the fractional ionization $x_e \equiv n_e/n_{\rm H}$. Molecular clouds may have a very low preshock fractional ionization, so that a modest amount of ionization in the shock can have a dramatic effect on the shock structure. There is even the possibility of a runaway: an increase in ionization enhances the heating rate through ion-neutral collisions, which causes the temperature to rise, and hence may further increase the ionization rate. Countervailing effects limit the magnitude of such runaways. Here we estimate the rates for various processes which could act to change the ionization.

Metal ions such as Na have a sufficiently low ionization energy that electron impact ionization is possible. We used thermal rates from Lotz (1967).

A more effective ionization process may be the emission of ultraviolet radiation in the shock which is able to photoionize trace metal atoms such as Na or Mg. Electron impact excitation of H Lyman alpha (Williams and Willis 1974) or H_2 Lyman band photons (Srivastava and Jensen 1977) are the principal sources of ultraviolet radiation. The resulting UV photons will be preferentially absorbed by dust: with a typical atomic photoionization cross section of $\sim 10^{-17}$ cm^2, a dust absorption cross section of $\sim 10^{-21}$ cm^2 per H nucleus (Savage and Mathis 1979), and an abundance ratio of $\sim 10^{-6}$ for the ionizable species, only $\sim 1\%$ of the photons are absorbed by metal atoms.

Ion-neutral collisions are a potential source of ionization, since the ions may be streaming through the neutral gas at tens of km s^{-1}; neutral-neutral collisions may also be important, since electrons and ions are so rare. Drawin (1968, 1969) has estimated the cross section for the reaction $A + A \rightarrow A^+ + e^- + A$ at low energies to be

$$\sigma(E) \approx \sigma_0 \left[\frac{E}{E_0} - 1 \right], \qquad E > E_0, \tag{25}$$

$$\sigma_0 = 7.67 \times 10^{-19} \left(\frac{I_{\rm H}}{I_{\rm A}} \right)^2 f_{\rm A} \ {\rm cm}^2, \tag{26}$$

$$E_0 = 2 I_{\rm A} \tag{27}$$

where E is the center-of-mass kinetic energy of A + A, $I_{\rm A}$ and $I_{\rm H}$ are the ionization potentials of A and H, respectively, and $f_{\rm A}$ is the oscillator strength for electric dipole transitions from the outermost shell of A to the continuum ($f = 0.665$ for H, $f \approx 1$ for H_2 and He). The generalization to the reaction

$$A + B \rightarrow A^+ + e^- + B \tag{28}$$

is unclear. We tentatively retain (25) and (26) for the cross section, and assume that the center of mass threshold energy (27) remains unchanged. Drawin's cross sectional estimate is based on classical arguments, and its accuracy, particularly near threshold, is highly uncertain. We note, however, that equations (25)–(27) are in fairly good agreement with low energy measurements on $He + He \rightarrow He^+ + e^- + He$ and $He + Ne \rightarrow He^+ + e^- + Ne$ down to $E \approx 60$ eV (Hayden and Utterback 1964), and in very good agreement with measured cross sections for $H + He \rightarrow H^+ + e^- + He$ down to $E = 40$ eV (Van Zyl and Utterback 1969; Van Zyl, Le, and Amme 1981). These experiments appear to support Drawin's estimate of $2I_{\rm A}$ for the threshold energy for (28), rather than $I_{\rm A}$ as would be suggested by energetic considerations alone.

If species A and B have kinetic temperatures $T_{\rm A}$ and $T_{\rm B}$ but are streaming through one another with relative drift velocity $v_{\rm AB}$, then the effective rate coefficient for (28) is

$$\langle \sigma v \rangle = \frac{\sigma_0}{x_0^2 s} \left(\frac{2kT_r}{\pi m_r} \right)^{1/2} \int_{x_0}^{\infty} dx\, x^2 \left(x^2 - x_0^2 \right) \left[e^{-(x-s)^2} - e^{-(x+s)^2} \right], \tag{29}$$

$$x_0^2 \equiv \frac{E_0}{kT_r}, \qquad s^2 \equiv \frac{m_r v_{\rm AB}^2}{2kT_r}, \tag{30}$$

$$m_r \equiv \frac{m_{\rm A} m_{\rm B}}{m_{\rm A} + m_{\rm B}}, \qquad T_r \equiv \frac{m_{\rm A} T_{\rm B} + m_{\rm B} T_{\rm A}}{m_{\rm A} + m_{\rm B}}. \tag{31}$$

We have used equation (29) to evaluate rate coefficients for the reactions $H_2 + I^+ \rightarrow H_2^+ + e^- + I^+$, $H + I^+ \rightarrow H^+ + e^- + I^+$, and $He + I^+ \rightarrow He^+ + e^- + I^+$.

When A and B are both neutral, the rate coefficient for (28) is obtained by setting $v_{AB} = 0$ in equation (29), obtaining rate coefficients

$$\langle \sigma v \rangle (H_2 + H_2 \rightarrow H_2^+ + e^- + H_2) = 9 \times 10^{-13} T_{n4}^{1/2} (1 + 0.028 T_{n4}) e^{-35.8/T_{n4}} \text{ cm}^3 \text{ s}^{-1}, \quad (32)$$

$$\langle \sigma v \rangle (H + H_2 \rightarrow H^+ + e^- + H_2) = 9 \times 10^{-13} T_{n4}^{1/2} (1 + 0.032 T_{n4}) e^{-31.6/T_{n4}} \text{ cm}^3 \text{ s}^{-1}, \quad (33)$$

$$\langle \sigma v \rangle (H + H \rightarrow H^+ + e^- + H) = 1.0 \times 10^{-12} T_{n4}^{1/2} (1 + 0.032 T_{n4}) e^{-31.6/T_{n4}} \text{ cm}^3 \text{ s}^{-1}, \quad (34)$$

where $T_{n4} \equiv T_n / 10^4$ K.

Ionization in slow heavy particle collisions may be created preferentially by the process

$$A + B \rightarrow A^+ + B^-. \quad (35)$$

Energetic considerations dictate a minimum threshold energy $E_0 = I_A - I_{B^-}$, where I_{B^-} is the electron affinity of B. In a further collision, B^- undergoes electron detachment ($A + B^- \rightarrow A + B + e^-$) or associative detachment ($A + B^- \rightarrow AB + e^-$). The limiting process is the reaction (35).

Measurements on $H_2 + H$ at low energies (Van Zyl and Utterback 1969; Van Zyl, Le, and Amme 1981) indicate $H_2 + H \rightarrow H_2^+ + H^-$ to be the dominant ionization channel at low energies. Cross sections between 20 and 100 eV can be fitted by

$$\sigma(E) \approx \sigma_0 (E/E_0 - 1)^2, \qquad E > E_0, \quad (36)$$

where $E_0 = 14.68$ eV is the minimum possible threshold energy, and $\sigma_0 = 9 \times 10^{-19}$ cm^2. The corresponding thermal rate coefficient is

$$\langle \sigma v \rangle (H_2 + H \rightarrow H_2^+ + H^-) \approx 2 \times 10^{-13} T_{n4}^{3/2} e^{-17.0/T_{n4}} (1 + 0.176 T_{n4}) \text{ cm}^3 \text{ s}^{-1}. \quad (37)$$

Whether reactions of the form (35) will be important for collision partners other than $H + H_2$ is not known.

The shock models reported in this paper were computed assuming constant fractional ionization. We have numerically computed, *a posteriori*, the change Δx_e in the fractional ionization due to the processes described above. The results are discussed in § X.

VI. MOLECULAR EXCITATION, DISSOCIATION, AND RADIATIVE COOLING

a) Excitation of Molecular Hydrogen

Inelastic collisions of H_2 molecules with neutral particles remove thermal energy from the neutral fluid at a rate

$$(G_n)_{H_2} = -n(H_2) \sum_i f_i \left[P_{ic} \langle E_{ic} \rangle_n + \sum_{j \neq i} P_{ij} (E_j - E_i) \right], \quad (38)$$

where the index i runs over all the rotation-vibration levels of H_2, f_i is the fractional population of level i, and E_i is its energy. The first term in brackets represents dissipation due to collision-induced dissociation from level i at a rate P_{ic} with an average energy loss of $\langle E_{ic} \rangle_n$ per dissociation. The other terms give the rate at which thermal energy is converted into the internal energy of H_2 and into H_2 quadrupole radiation in terms of P_{ij}, the rate of transitions from level i to level j induced by collisions with neutral particles. The cooling of the electron fluid by inelastic electron–H_2 collisions is given by

$$(G_e)_{H_2} = -n(H_2) \sum_i f_i \left[Q_{ic} \langle E_{ic} \rangle_e + \sum_{j \neq i} Q_{ij} (E_j - E_i) \right], \quad (39)$$

in which the neutral impact transition rates have been replaced by rates Q_{ij} for transitions produced by collisions with electrons.

For the preshock conditions that we studied, the level populations of H_2 attain a steady state on a time scale much shorter than the average time between dissociative collisions. The f_i are therefore the solutions of the equations of

statistical equilibrium,

$$f_i\left[\sum_{j\neq i}(P_{ij}+Q_{ij})+\sum_{j<i}A_{ij}\right]=\sum_{j\neq i}f_j(P_{ji}+Q_{ji})+\sum_{j>i}f_jA_{ji}, \quad (40)$$

in which the depopulation of bound levels by collision-induced dissociation has been neglected and where A_{ij} is the Einstein A-coefficient for the electric quadrupole transition connecting levels i and j. Because few of the collision rates that appear in the equations have been measured or calculated, we further simplify the problem by writing each level population as the product of independent vibrational and rotational distributions.

We have calculated the rotational distribution including processes in which the rotational quantum number J changes by ± 2 and the ratio of ortho- to para-hydrogen is fixed at 3. The energies of levels with $J=0$ to $J=21$ were obtained from ab initio calculations of Waech and Bernstein (1967), which agree well with measured wavelengths of transitions in the pure rotation band of H_2 (Cooper, May, and Gupta 1970; Reid and McKellar 1978; Beck, Lacy, and Geballe 1979; Knacke and Young 1981). A-values were obtained from Turner, Kirby-Docken, and Dalgarno (1977).

Rates for excitation of H_2 by collisions with electrons, H and He atoms, and H_2 molecules were obtained (using the principle of detailed balance) from the de-excitation rates in Tables 1 and 2. Cross sections for rotational excitation by electrons have been measured for $J=0\rightarrow 2$ (Crompton, Gibson, and McIntosh 1969) and $J=1\rightarrow 3$ (Linder and Schmidt 1971). The experimental excitation cross sections for $E\lesssim 5$ eV may be approximated by Born-quadrupole cross sections (Gerjuoy and Stein 1955) but with an effective quadrupole moment $1.53(E/\mathrm{eV})^{1/4}ea_0^2$; the correspond-

TABLE 1

RATE COEFFICIENTS FOR $M+H_2(v,J_u)\rightarrow M+H_2(v,J_l)$

M	$J_u\rightarrow J_l$	$\langle\sigma v\rangle(\mathrm{cm^3\,s^{-1}})$	Notes
e.....	$J\rightarrow J-2$	$1.0\times10^{-10}[J(J-1)/(2J+1)](1+1.5/x)$	1
H	$J\rightarrow J-2$	$4.6\times10^{-12}(2J-1)T_n^{1/2}(1+x)^{1/2}e^{-[5.01x+0.1187(4J-2)]}$	1
H_2 ...	$2\rightarrow 0$	$4\times10^{-14}T_n^{3/4}$	
H_2 ...	$3\rightarrow 1$	$5\times10^{-15}T_n$	
H_2 ...	$J\rightarrow J-2$	$1\times10^{-10}\alpha((2J-3)/(2J+1))\exp[-5x^4/(1+x^4)]$ $(J>3)$	1,2
H_2 ...	$J\rightarrow J-4$	$3\times10^{-11}\alpha((2J-7)/(2J+1))\exp(-2x)$	1,2
H_2 ...	$J\rightarrow J-6$	$2\times10^{-11}\alpha((2J-11)/(2J+1))\exp(-2x)$	1,2
He ...	$J\rightarrow J-2$	$1\times10^{-10}((2J-3)/(2J+1))\exp[-5x^4/(1+x^4)]$	1
He ...	$J\rightarrow J-4$	$3\times10^{-11}((2J-7)/(2J+1))\exp(-2x)$	1
He ...	$J\rightarrow J-6$	$2\times10^{-11}((2J-11)/(2J+1))\exp(-2x)$	1

NOTES.—(1) $x\equiv[E(v,J_u)-E(v,J_l)]/kT$. (2) $\alpha=4$ is recommended (see text).

TABLE 2

RATE COEFFICIENTS FOR $M+H_2(v_u)\rightarrow M+H_2(v_l)$

M	$v_u\rightarrow v_l$	$\langle\sigma v\rangle(\mathrm{cm^3\,s^{-1}})$	Notes
e.....	$v\rightarrow v-1$	$3.7\times10^{-11}T_e^{1/2}(1+x/2)^{-1}$	1
e.....	$v\rightarrow v-2$	$2.5\times10^{-12}T_e^{1/2}(1+x/2)^{-1}$	1
e.....	$v\rightarrow v-3$	$2.5\times10^{-13}T_e^{1/2}(1+x/2)^{-1}$	1
H	$1\rightarrow 0$	$1.0\times10^{-12}T_n^{1/2}e^{-1000/T_n}$	
H	$2\rightarrow 0$	$1.6\times10^{-12}T_n^{1/2}e\exp[-(400/T_n)^2]$	
H	$2\rightarrow 1$	$4.5\times10^{-12}T_n^{1/2}\exp[-(500/T_n)^2]$	
H_2 ...	$1\rightarrow 0$	$6.6\times10^{-14}T_n\exp(-79.99/T_n^{1/3})/(1-e^{-\Theta/T_n})$	2
H_2 ...	$v\rightarrow v-\Delta v$	$\langle\sigma v\rangle_{1\rightarrow 0}\left[\frac{1+1.64x}{1+1.64x/\Delta v}\right]^{3/2}\exp\left[\frac{1.5\Theta}{\Theta+T_n}(1-\Delta v)\right]$	1,2
He ...	$1\rightarrow 0$	$1.3\times10^{-13}T_n\exp(-95.21/T_n^{1/3})/(1-e^{-\Theta/T_n})$	2
He ...	$v\rightarrow v-\Delta v$	$\langle\sigma v\rangle_{1\rightarrow 0}\left[\frac{1+1.64x}{1+1.64x/\Delta v}\right]^{3/2}\exp\left[\frac{1.5\Theta}{\Theta+T_n}(1-\Delta v)\right]$	1,2

NOTES.—(1) $x\equiv[E(v_u)-E(v_l)]/kT\approx(v_u-v_l)\Theta/T$. (2) $\Theta=5987$ K.

ing de-excitation rates are given in Table 1. Cross sections for rotational excitation by H were obtained from the "surprisal analysis" fit of Elitzur and Watson (1978). Important uncertainties in the values persist (cf. Green and Truhlar 1979). Rates for $J = 2 \rightarrow 0$ and $J = 3 \rightarrow 1$ de-excitation by H_2 were chosen to match the accurate quantum calculations of Monchick and Schaefer (1980) for collisions with H_2 in the $J = 1$ state, and to have reasonable extrapolations for $T_n < 10^4$ K. The rates for rotational de-excitation by He, or of levels with $J > 3$ by H_2, were chosen to be proportional to the He–H_2 rates computed by Green, Ramaswamy, and Rabitz (1978) for $J < 8$ and by Tarr and Rabitz (1978) for $J < 19$ at $T_n = 3000$ K (H_2–H_2 rates are expected to be at least as large as He–H_2 rates). The coefficient of proportionality has been assumed to be $\alpha = 4$ in the present work; this is only an educated guess, and further experimental or theoretical work on H_2–H_2 collisional excitation cross sections is urgently needed.

We calculated the vibrational distribution by collapsing the rotational levels into one state for each vibrational level from $v = 0$ to $v = 14$. As an average over J we used the A-coefficients for the $O(2)$ lines connecting each pair of vibrational levels. Rate constants for collisional excitation from $v = 0$ to $v = 1$ were derived from the cross sections of Ehrhardt *et al.* (1968) for excitation by electron impact. For vibrational excitation by H atom impact we use the rates of Hollenbach and McKee (1979), which are based on cross sections calculated by Chu (1979). The rates for de-excitation of $v = 1$ by vibrational-translational energy transfer in collisions with other H_2 molecules and with He are from laboratory measurements by Dove and Teitelbaum (1974). For vibrational transitions between other levels, we estimate rates using the "surprisal analysis" of Procaccia and Levine (1975) for rigid-rotor harmonic oscillators (our fit is based on approximating the modified Bessel function $K_2(x) \approx [2^{2/3} + (\pi/2)^{1/3}x]^{3/2}x^{-2}e^{-x}$, and approximating their parameter $\lambda_v \approx 1.5/[1 + \Theta/T]$).

At low particle densities, the vibrational distribution decreases rapidly with increasing v, and collisions with $\Delta v > 1$ dominate the excitation to levels with $v > 1$. In order to ensure that the cooling rate is calculated accurately at low densities, we have included the effects of collisions with $\Delta v > 1$ on the populations of levels with $v < 3$.

b) Dissociation of Molecular Hydrogen

Collision-induced dissociation cools the neutral gas and increases its number density at a rate

$$(N_n)_{H_2} = n(H_2)\sum_i f_i(Q_{ic} + P_{ic}). \tag{41}$$

The dissociation of H_2 molecules by electron impact is discussed in § IV. Collision-induced dissociation of H_2 by neutral particle impact can occur from any initial level i by a transition to the vibrational continuum of the ground electronic state. However, the transition rates P_{ic} decrease rapidly with decreasing v (Blais and Truhlar 1982). We employ a kinetic model in which dissociation occurs by excitation from the $v = 14$ state (Dalgarno and Roberge 1979; Roberge and Dalgarno 1982). At laboratory densities the model reproduces, by construction, the measured rate constants for collisional dissociation (Breshears and Bird 1973). It predicts a rapid decrease in the dissociation rates at particle densities below 10^5 cm^{-3}, as radiative stabilization depopulates the excited vibrational levels.

In addition to dissociation due to thermal collisions with neutrals or electrons, there can also be a contribution due to collisions with streaming ions: $H_2 + I^+ \rightarrow H + H + I^+$. To estimate the rate coefficient for this ion-molecule reaction, we assume that a fraction γ of "orbiting" collisions with a center-of-mass energy in excess of the threshold energy $E_0 = 4.48$ eV lead to dissociation. The cross section is then

$$\sigma(E) = \sigma_0(E_0/E)^{1/2} \quad \text{for } E > E_0, \tag{42}$$

$$\sigma_0 = 2\pi\gamma a_0^2\left(\frac{\alpha}{a_0^3}\right)^{1/2}\left(\frac{I_H}{E_0}\right)^{1/2}, \tag{43}$$

where $\alpha = 5.42a_0^3$ is the polarizability of H_2, and $I_H = 13.6$ eV is the ionization energy of atomic hydrogen. We have assumed $\gamma = 1$ (presumably an upper limit) in the present calculations.

If the ions and neutrals each have Maxwellian velocity distributions but a relative streaming velocity v, then the above cross section results in a rate coefficient given by

$$\langle \sigma v \rangle = \frac{\sigma_0 x_0}{s}\left(\frac{2kT_r}{\pi m_r}\right)^{1/2}\int_{x_0}^{\infty} dx\, x\left[e^{-(x-s)^2} - e^{-(x+s)^2}\right] \tag{44}$$

$$\approx \sigma_0 x_0\left(\frac{8kT_r}{\pi m_r}\right)^{1/2}\left(\frac{\pi}{4} + z\right)^{1/2}e^{-z}, \tag{45}$$

$$x_0^2 \equiv \frac{E_0}{kT_r}, \qquad s^2 \equiv \frac{m_r v^2}{2kT_r}, \tag{46}$$

$$m_r \equiv \frac{2m_I m_{\rm H}}{m_I + 2m_{\rm H}}, \qquad T_r \equiv \frac{m_I T_n + 2m_{\rm H} T_i}{m_I + 2m_{\rm H}}, \tag{47}$$

$$z \equiv \frac{x_0^2}{1 + \frac{1}{2}s^2}. \tag{48}$$

The approximation (45) is accurate to within a factor of 2 for $x_0 \leqslant 3.5$. We use equation (45) to estimate the rate for ion-impact dissociation of H_2.

It is also possible for H_2 dissociation to occur as a result of collisions with streaming dust grains. The probability of dissociation in an impact at a given impact energy E is not known; we arbitrarily assume it to be simply $(1 - 4.48\text{eV}/E)$.

c) CO, OH, *and* H_2O

The permitted rotational lines of CO, OH, and H_2O make a substantial contribution to the cooling in the shock waves considered here. We have used the formalism and data of Hollenbach and McKee (1979) to estimate their contribution to the cooling except for the following: (i) To compute the effective optical depth τ_T, we assumed that the local velocity gradient is large enough that it, rather than thermal broadening, determines the escape probability. Thus we have made a Sobolev-like approximation, and taken τ_T to be

$$\tau_T = 3.39 \times 10^{-2}\ \text{cm}^3\ \text{K}^3\ n(\text{X})\, A_0 \left[\eta_T (E_0/k)^2 T_n \nabla\right]^{-1}, \tag{49}$$

where $n(\text{X})$ is the local number density (X = CO, OH, or H_2O), the constants E_0/k, A_0, and η_T are taken from Table 3 of Hollenbach and McKee (1979), and ∇ is the effective velocity gradient, taken to be the larger of $|dv_n/dz|$ and $10^{-13}\ \text{s}^{-1}$ in order that the unperturbed cloud (with $dv_n/dz = 0$ in our idealization) have a finite optical depth so that CO may act as a coolant. (ii) For CO, we have used the expression for the critical density given by McKee *et al.* (1982). (iii) In the case of H_2O, we have, following the recommendation of Hollenbach and McKee (1981), reduced the final H_2O cooling rate by a factor of 3.

VII. OXYGEN-BASED CHEMISTRY

Though not abundant in the preshock gas, H_2O can be produced rapidly from O or OH by endothermic reactions once the gas temperature rises above a few hundred degrees. The chemistry of any gas-phase oxygen which is not in CO is determined primarily by the reaction network linking the four species O, OH, H_2O, and O_2. In the dark clouds where stellar ultraviolet radiation is absent, photochemistry and ion-molecule reactions in the shocked gas are unimportant unless the shocked gas itself emits appreciably in the ultraviolet. The present study is restricted to shocks in which T_n and T_e never rise above about 10^4 K, and the oxygen chemistry is determined essentially by the reactions involving H, H_2, and neutral molecules containing oxygen (cf. Aannnestad 1973; Iglesias and Silk 1978; Elitzur and de Jong 1978). The reactions and their rate coefficients are (cf. Hollenbach and McKee 1979):

$$\text{H}_2 + \text{O} \rightarrow \text{OH} + \text{H}\text{:}\ k = 3 \times 10^{-14}\, T_n \exp\left(-4480/T_n\right)\ \text{cm}^3\ \text{s}^{-1}, \tag{50}$$

$$\text{H} + \text{OH} \rightarrow \text{H}_2 + \text{O}\text{:}\ k = 1.4 \times 10^{-14}\, T_n \exp\left(-3500/T_n\right)\ \text{cm}^3\ \text{s}^{-1}, \tag{51}$$

$$\text{H}_2 + \text{OH} \rightarrow \text{H}_2\text{O} + \text{H}\text{:}\ k = 3.6 \times 10^{-11} \exp\left(-2590/T_n\right)\ \text{cm}^3\ \text{s}^{-1}, \tag{52}$$

$$\text{H} + \text{H}_2\text{O} \rightarrow \text{H}_2 + \text{OH}\text{:}\ k = 1.5 \times 10^{-10} \exp\left(-10250/T_n\right)\ \text{cm}^3\ \text{s}^{-1}, \tag{53}$$

$$\text{H} + \text{O}_2 \rightarrow \text{O} + \text{OH}\text{:}\ k = 3.7 \times 10^{-10} \exp\left(-8450/T_n\right)\ \text{cm}^3\ \text{s}^{-1}, \tag{54}$$

$$\text{OH} + \text{OH} \rightarrow \text{H}_2\text{O} + \text{O}\text{:}\ k = 1.0 \times 10^{-11} \exp\left(-550/T_n\right)\ \text{cm}^3\ \text{s}^{-1}, \tag{55}$$

$$\text{OH} + \text{O} \rightarrow \text{O}_2 + \text{H}\text{:}\ k = 4 \times 10^{-10} \exp\left(-600/T_n\right)\ \text{cm}^3\ \text{s}^{-1}. \tag{56}$$

Dissociation of OH, O_2, and H_2O by collisions with streaming ions was also included. Rates for $I^+ + OH \rightarrow I^+ + O + H$ and $I^+ + O_2 \rightarrow I^+ + O + O$ were computed using equations (42)–(45), with an assumed polarizability $\alpha = 5a_0^3$, $\gamma = 1$, and threshold energies $E_0 = 4.39$ eV and 5.20 eV, respectively. In the case of $I^+ + H_2O$ there are two dissociating channels, leading to $I^+ + H_2 + O$ ($E_0 = 5.03$ eV) and $I^+ + OH + H$ ($E_0 = 5.12$ eV). For these two channels let the effective values of γ in equation (43) be γ_1 and γ_2, respectively. We have taken $\alpha = 5a_0^3$, and assumed $(\gamma_1, \gamma_2) = (0, 1)$ for initial center-of-mass energies $5.03 < E < 5.12$ eV, and $(\gamma_1, \gamma_2) = (1/2, 1/2)$ for $E > 5.12$ eV.

VIII. REMOVAL OF GRAIN MANTLES

The gas-phase abundances depend on the degree to which atoms and molecules which have been depleted by accretion onto dust grains in the preshock gas are restored to the gaseous phase during the passage through the shock by thermal sublimation, photodesorption, grain-grain collisions, and sputtering.

Hollenbach and McKee (1979) have discussed the efficacy of thermal sublimation, photodesorption, and sputtering of grains in nonmagnetic shock waves. Thermal sublimation and photodesorption are found to be quite effective in high-density nonmagnetic shocks, because the postshock gas is heated to temperatures $T_s \approx 5 \times 10^3 \, (v_s/10 \text{ km s}^{-1})^2$ K and heats the dust both by direct collisions and by emitting optical and ultraviolet radiation which is absorbed by the dust. In the MHD shock waves considered here, however, most of the radiation emitted by the shocked gas is in the infrared and is ineffective at heating the grains because of the reduced grain opacity at these wavelengths.

Collisional heating alone will heat the grains to a temperature

$$T_{\rm gr} = \left[n_n (2kT_n/\pi\mu_n)^{1/2} kT_n/\alpha Q \right]^{1/4}, \tag{57}$$

where Q, the Planck-averaged emissivity, may be approximated by $Q = T_{\rm gr}^{3/2}(a/\text{cm})$ (Draine 1981), a is the grain radius, and the accommodation coefficient $\alpha \approx 1/2$. Thus

$$T_{\rm gr} = 15 \left(n_{\rm H}/10^6 \text{ cm}^{-3} \right)^{2/11} \left(4 \times 10^{-5} \text{ cm}/a \right)^{2/11} \left(T_n/10^3 \text{ K} \right)^{3/11} \text{K}. \tag{58}$$

Since grain temperatures $T_{\rm gr} = 100$ K are required to sublime one monolayer of H_2O ice in a year, shocks in which $n_{\rm H} \lesssim 10^7$ cm^{-3} and $T_n \lesssim 5000$ K will not result in appreciable thermal sublimation of H_2O ice mantles.

Sputtering of volatile mantles can be important. The dust grains will be closely coupled to the magnetic field B provided $\omega\tau \gtrsim 1$, where ω is the cyclotron frequency and τ is the collisional damping time (cf. Draine 1980). If we neglect the orbital motion of the grains around the field lines (see the remarks in § X on betatron acceleration), then the velocity of the grains with respect to the neutral gas is

$$u = (v_n - v_i)\omega\tau / \left[1 + (\omega\tau)^2 \right]^{1/2}, \tag{59}$$

and the erosion rate due to neutral species X is approximately (Draine and Salpeter 1979*a*)

$$\frac{da}{dt} \approx -\frac{\Omega}{4} n_{\rm X} \left(u^2 + 8kT_n/\pi m_{\rm X} \right)^{1/2} Y_{\rm X}(\bar{E}), \tag{60}$$

where $\bar{E} \equiv m_x u^2/2 + 2kT_n$, $Y_{\rm X}(E)$ is the sputtering yield (H_2O molecules per impact) for an atom or molecule X impinging with a kinetic energy E, and Ω is the volume per molecule. Equation (62) is valid provided the typical impact energy $\bar{E}$ is well in excess of the sputtering threshold (Draine and Salpeter 1979*a*); this criterion is satisfied in all of the present models in which sputtering turns out to be significant. The net erosion of a grain after passage through the shock is

$$\Delta a = \int (v_n - u)^{-1} \frac{da}{dt} dz. \tag{61}$$

We computed Δa for grains of initial radius 4×10^{-5} cm, using the sputtering yield for H_2O ice from Draine and Salpeter (1979a).

Grain-grain collisions may be important under some conditions (cf. § X) but have not been included in the present study.

IX. PRESHOCK CONDITIONS

a) *Composition*

For the unperturbed preshock gas we have adopted the composition shown in Table 3. The CO abundance is a compromise between the results of Dickman (1978) and Frerking, Langer, and Wilson (1982). Carbon monoxide and atomic carbon were assumed to have comparable abundances, as indicated by the recent observations of Phillips and Huggins (1981) for dense clouds, and 80% of the total carbon is taken to be depleted into or onto grains. The initial O I abundance is taken to be 50% of the cosmic abundance (Meyer 1979), 6% of the oxygen is in CO, 20% is in silicate grain cores, and the remaining 24% is in icy grain mantles.

Measurements of the wavelength dependence of interstellar extinction and polarization (e.g., Carrasco, Strom, and Strom 1973) suggest that grains in dense clouds are somewhat larger than those in more diffuse parts of the interstellar medium, presumably as the result of both coagulation and mantle growth in the molecular cloud. We have assumed a characteristic grain radius $a = 4 \times 10^{-5}$ cm and grain abundance $2.5 \times 10^{-14} n_{\rm H}$; with a grain density 2.5 g cm^{-3}, this corresponds to a grain to hydrogen mass ratio of 0.010.

We have considered three densities for the preshock gas: $n_{\rm H} = 10^2$ cm^{-3}, corresponding to a diffuse molecular cloud, $n_{\rm H} = 10^4$ cm^{-3}, corresponding to a dark molecular cloud; and $n_{\rm H} = 10^6$ cm^{-3}, corresponding to the dense core of a star-forming molecular cloud.

The fractional ionization in the preshock gas depends upon the density. In diffuse molecular clouds, ambient ultraviolet radiation ionizes the metals and we adopted a fractional ionization of 10^{-4} for the $n_{\rm H} = 10^2$ cm^{-3} models. Within denser clouds dust attenuates the incident radiation and cosmic rays produce most of the ionizing events. For the dense cloud models with $n_{\rm H} = 10^4$ and 10^6 cm^{-3} we adopted a fractional ionization

$$x_e \equiv n_e / n_{\rm H} = 1 \times 10^{-5} \left(n_{\rm H} / {\rm cm}^{-3} \right)^{-1/2}, \tag{62}$$

which appears to be consistent with both recent observational studies (Guélin *et al.* 1977; Watson, Snyder, and Hollis 1978; Turner and Zuckerman 1978; Wootten, Snell, and Glassgold 1979; Guélin, Langer, and Wilson 1982) and theoretical investigations (Elmegreen 1979; de Jong, Dalgarno, and Boland 1980; Umebayashi and Nakano 1980; Graedel, Langer, and Frerking 1982) for the assumed primary ionization rate $\zeta = 10^{-17}$ s^{-1} adopted here.

The molecular hydrogen fraction in the preshock gas was determined by equating the rate of formation of H_2 on grains, $10^{-17} n_{\rm H} n({\rm H}) {\rm cm}^3$ s^{-1}, to the rate at which cosmic rays dissociate H_2. The corresponding atomic hydrogen fractions are given in Table 3.

The assumed grain temperatures in Table 3 are somewhat higher than those appropriate for grains heated by the average radiation field in the Galaxy, and are intended to be appropriate to matter in the vicinity of star-forming regions. The temperature in the preshock gas, obtained by balancing heating and cooling, is given in Table 3 for each of the three densities considered.

b) *Magnetic Field*

The magnetic field strength in the preshock gas is a critical parameter. Heiles (1976) and Verschuur (1979) have reviewed the observational data. In many cases only upper limits to the field strength are available, but it appears that

TABLE 3

PRESHOCK CONDITIONS

Quantity	Diffuse Cloud	Dark Cloud	Dense Cloud Core
$n_{\rm H}$ (cm^{-3})	1×10^2	1×10^4	1×10^6
$x_e = n_e / n_{\rm H}$	1×10^{-4}	1×10^{-7}	1×10^{-8}
B_0 (gauss), standard	1×10^{-5}	1×10^{-4}	1×10^{-3}
B_0 (gauss), weak	...	5×10^{-5}	5×10^{-4}
$n({\rm H})/n_{\rm H}$	2.96×10^{-2}	3.05×10^{-4}	3.05×10^{-6}
$n({\rm CO})/n_{\rm H}$	5×10^{-5}	5×10^{-5}	5×10^{-5}
$n({\rm C})/n_{\rm H}$	5×10^{-5}	5×10^{-5}	5×10^{-5}
$n({\rm O})/n_{\rm H}$	4.25×10^{-4}	4.25×10^{-4}	4.25×10^{-4}
$n({\rm grain})/n_{\rm H}$	2.5×10^{-14}	2.5×10^{-14}	2.5×10^{-14}
a(cm)	4×10^{-5}	4×10^{-5}	4×10^{-5}
$T_{\rm grain}$(K)	30	40	50
ζ(s^{-1})	1×10^{-17}	1×10^{-17}	1×10^{-17}
T_n(K)	19.6	8.4	26.7

field strengths B_0 of about 10 microgauss may be appropriate for diffuse clouds. Zeeman observations at 21 cm have indicated line-of-sight field strengths of up to 50 microgauss for dense H I clouds, and OH masers in dense molecular clouds show Zeeman splitting indicating field strengths within the masing region of several milligauss. Observations of polarized infrared emission from some dense clouds indicate that the emitting dust grains are highly aligned (the BN–KL region in Orion is a prominent example); if the alignment is produced by the Davis-Greenstein mechanism, milligauss magnetic field strengths are called for (Dyck and Beichman 1974; Dennison 1977; Johnson *et al.* 1981), even if the grains are in superthermal rotation (Purcell 1979).

The observational data are consistent with an ambient magnetic field strength in molecular clouds scaling roughly as

$$B_0 \approx b_0 \left(n_{\rm H}/{\rm cm}^{-3} \right)^{1/2}, \tag{63}$$

with $b_0 \approx 1$ microgauss. The recent upper limits on molecular cloud magnetic fields found by Crutcher, Troland, and Heiles (1981) are not inconsistent with this estimate when uncertainties in the density and projection effects are allowed for.

As the standard case we have used (63) with $b_0 = 1$ microgauss; we have also considered weak field cases with $b_0 = 0.5$ microgauss to assess the sensitivity of our results to the magnetic field strength and to allow for cases where the shock velocity is not perpendicular to the magnetic field. For the standard magnetic field, the Alfvén velocity for long wavelength hydromagnetic waves is $v_{\rm A} = 1.85$ km s^{-1}; for the weak field case $v_{\rm A} = 0.93$ km s^{-1}.

X. MODEL SHOCK WAVES

a) *Computational Methods*

In *C*-type shock waves, the hydrodynamic variables are all continuous and calculation of the shock structure can be posed as an initial value problem. We specify the preshock density $n_{\rm H}$, fractional ionization x_e, and grain temperature $T_{\rm gr}$, and obtain steady state solutions for the temperatures (T_n, T_i, and T_e) and the atomic hydrogen fraction $n({\rm H})/n_{\rm H}$. Then, for a specified magnetic field B_0 and shock speed v_s, we assume the neutral gas velocity v_n (in the frame of reference where the shock is stationary) to have been disturbed by a small amount: $v_n = v_s(1+u)$, with, typically, $u = -10^{-5}$. We then use the linearized hydrodynamic equations to obtain the perturbations in v_i, T_n, T_i, and T_e (Draine 1980), which then provide the starting point for a numerical integration of equations (1)–(9). Because of the multiple length scales characterizing the differential equations, we have employed the integration technique developed by Gear (1971) for stiff differential equations. In computing the hydrodynamics, the fractional ionization x_e and ionic molecular weight μ_i were assumed to remain constant through the shock. The oxygen chemistry was also integrated numerically in parallel with the hydrodynamics, with the local concentrations of O, OH, and H_2O used in computing the radiative cooling rates.

The integration scheme is successful only for *C*-type shocks, for which the neutral gas flow is everywhere supersonic. If the preshock conditions are such that the shock is *J*-type, the numerical integration causes the neutral flow speed v_n to become transonic, at which point the expression for dv_n/dz becomes singular and the integration breaks down.

We have investigated six sets of preshock conditions, corresponding to the weak and strong B field cases for $n_{\rm H} = 10^2$, 10^4, and 10^6 cm^{-3}. We discovered that the $n_{\rm H} = 10^2$ cm^{-3} weak B field case admitted only *J*-type shocks, at least for $v_s > 5$ km s^{-1}, whereas in the other five cases the shocks were *C*-type over the velocity range considered.

For each of the five preshock conditions which admitted *C*-type shocks, we have computed a sequence of shock models, beginning with a shock speed $v_s = 5$ km s^{-1} and increasing the shock speed in steps up to a maximum shock speed $v_{\rm crit}$ such that one of the following situations occurs: (1) The peak value of the neutral gas temperature in the shock exceeds 10^4 K, in which case our treatment of H_2 collisional excitation and dissociation is of questionable validity. (2) The H_2 is fully dissociated, in which case a slight further increase in shock speed leads to a dramatic increase in the peak temperature, since a major coolant is destroyed. (3) The change in fractional ionization Δx_e (computed *a posteriori*) is large enough to change F_n, the force/volume on the neutral gas, by more than 10% in the hottest part of the shock. Condition (3) can be restated as

$$\Delta x_e > 0.1\{1 + [(F_n)_d/(F_n)_i]_{\rm max}\} x_{e0}, \tag{64}$$

where $[(F_n)_d/(F_n)_i]$ is the ratio of the momentum transfer rate due to neutral-dust grain collisions to that due to ion-neutral collisions, evaluated at the hottest point in the shock. (4) The shock becomes *J*-type.

We list the critical shock speed $v_{\rm crit}$ in Table 4. Different phenomena determine $v_{\rm crit}$ for the different preshock conditions examined. In the $n_{\rm H} = 10^2$ cm^{-3} diffuse cloud models, the limiting shock speed $v_{\rm crit}$ is determined by the

TABLE 4

CRITICAL SHOCK SPEED v_{crit}

PRESHOCK CONDITIONS				
$n_H(cm^{-3})$	x_e	B_0(gauss)	v_{crit}(km s^{-1})	BEHAVIOR FOR $v_s \geq v_{crit}$
10^2.....	10^{-4}	1×10^{-5}	25	Shock becomes J-type
10^4.....	10^{-7}	5×10^{-5}	46	Self-ionization: $\Delta x_e > 4\times10^{-8}$
		1×10^{-4}	49	Self-ionization: $\Delta x_e > 4\times10^{-8}$
10^6.....	10^{-8}	5×10^{-4}	40	H_2 dissociation
		1×10^{-3}	44	H_2 dissociation

transition of the shock models from C-type to J-type as the shock speed is increased. For the $n_H = 10^4$ cm^{-3} models, self-ionization was responsible for v_{crit}; of the ionization mechanisms discussed in § V, the most important in the shocks considered here were found to be collisional ionization of H_2 and He by streaming ions, and electron impact ionization of trace metals. For the $n_H = 10^6$ cm^{-3} models, v_{crit} was established by the dissociation of the molecular hydrogen at high shock speeds.

b) Results and Discussion

i) Shock Structure

The general character of the shock structure is illustrated in Figures 1–3 which contain hydrodynamic profiles of $v_s = 25$ km s^{-1} shock waves propagating into $n_H = 10^2$, 10^4, and 10^6 cm^{-3} molecular gas with the standard magnetic

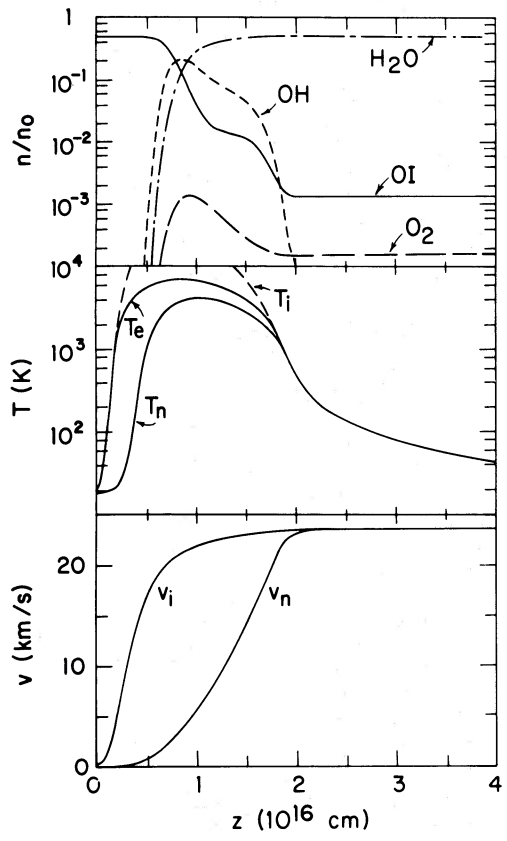

FIG. 1

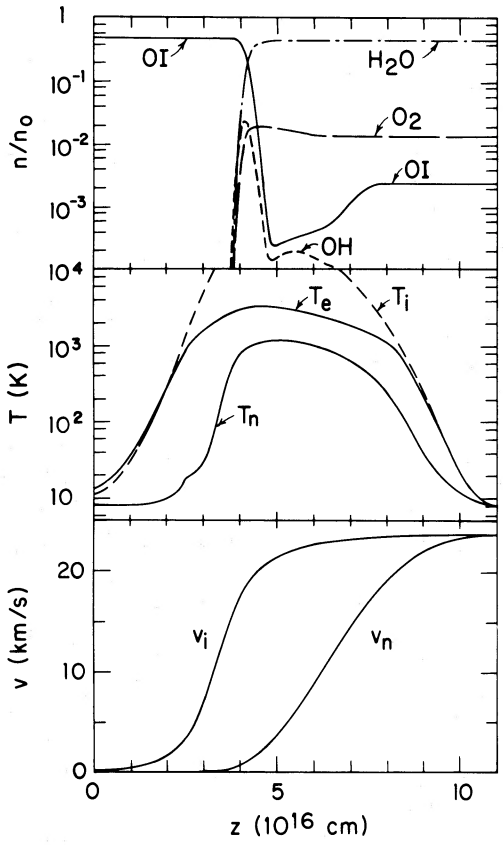

FIG. 2

FIG. 1.—Structure of a $v_s = 25$ km s^{-1} shock in a diffuse molecular cloud with $n_H = 10^2$ cm^{-3}, $x_e = 10^{-4}$, and $B_0 = 10$ μG. The quantities v_n and v_i are here measured relative to the preshock gas.

FIG. 2.—Structure of a $v_s = 25$ km s^{-1} shock in a molecular cloud with $n_H = 10^4$ cm^{-3}, $x_e = 10^{-7}$, and $B_0 = 100$ μG.

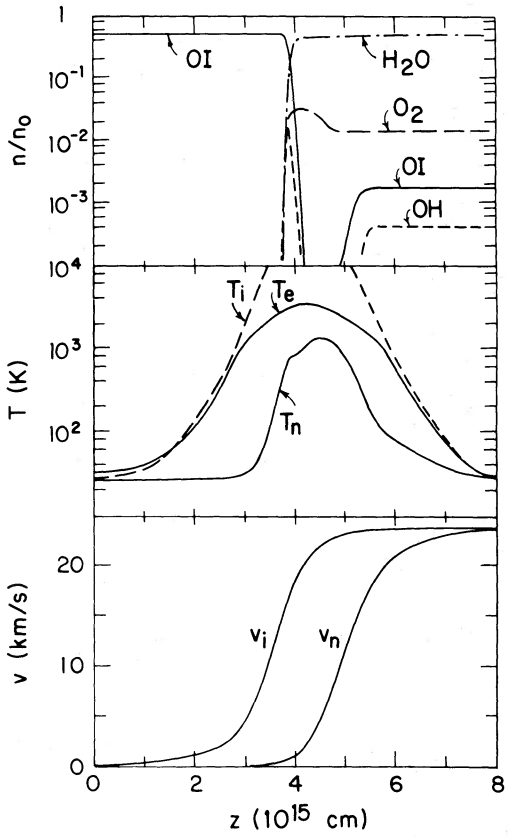

FIG. 3.—Structure of a $v_s = 25$ km s^{-1} shock in a dense molecular cloud with $n_H = 10^6$ cm^{-3}, $x_e = 10^{-8}$, and $B_0 = 1.0$ mG

fields $B_0 = 10^{-5}$, 10^{-4}, and 10^{-3} gauss, respectively. In all three cases the maximum value of the neutral temperature (4297 K, 1223 K, and 1334 K) is far below the shock temperature $T_s \approx 3\mu v_s^2/16k \approx 3.3 \times 10^4$ K resulting from a nonmagnetic shock. Consequently there is negligible dissociation of the molecular hydrogen in these 25 km s^{-1} shock waves, whereas nonmagnetic shock models for preshock densities $n_H \gtrsim 10^4$ cm^{-3} (Kwan 1977; London, McCray, and Chu 1977; Hollenbach and McKee 1980) predict complete dissociation of hydrogen for $v_s \gtrsim 24$ km s^{-1}.

ii) *Cooling Mechanisms*

In order to make clear the dominant cooling processes, Figure 4 shows the quantity $8\pi I/\rho_0 v_s^3$ for each of the important coolant species, where $4\pi I$ is the total power per surface area emitted by a given coolant species. Since the total power per unit area radiated by the shock is approximately $\frac{1}{2}\rho_0 v_s^3$, the quantity plotted in Figure 4 is effectively the fraction of the total cooling contributed by each of the species shown. We note that for the diffuse cloud shocks ($n_H = 10^2$ cm^{-3}) H_2 is the dominant coolant over the entire range of shock speeds considered. For the $n_H = 10^4$ cm^{-3} case, H_2 is the dominant coolant for $v_s > 11$ km s^{-1}, but for $5 < v_s < 11$ km s^{-1} the fine-structure lines of O I are more effective. For $v_s > 15$ km s^{-1}, the neutral temperature rises above ~ 500 K in the shock, and endothermic reactions convert much of the O I into OH and H_2O. The O I contribution to the cooling drops off and the rotational lines of H_2O begin to contribute strongly. For the $n_H = 10^6$ cm^{-3} case, O I is the dominant coolant for $v_s < 12$ km s^{-1}, but for $v_s \gtrsim 12$ km s^{-1} the O I is converted into H_2O, which then dominates the cooling. The H_2 contribution to the cooling increases rapidly for $v_s > 20$ km s^{-1} as the neutral temperature rises above ~ 1000 K in these shocks and the vibrational levels of H_2 begin to be appreciably excited, but most of the cooling power is in H_2O rotational lines for $12 < v_s < 40$ km s^{-1}.

A temperature of about 500 K is required for the endothermic reactions that produce H_2O to proceed rapidly. The neutral temperature profile in Figure 3 reflects this: with the onset of appreciable ion-neutral slip at $z \approx 3 \times 10^{15}$ cm behind the front in Figure 3, the neutral temperature begins to rise rapidly until it reaches ~ 800 K, at which point H_2O has become abundant and dramatically enhances the radiative cooling. The temperature shoulder at ~ 800 K is

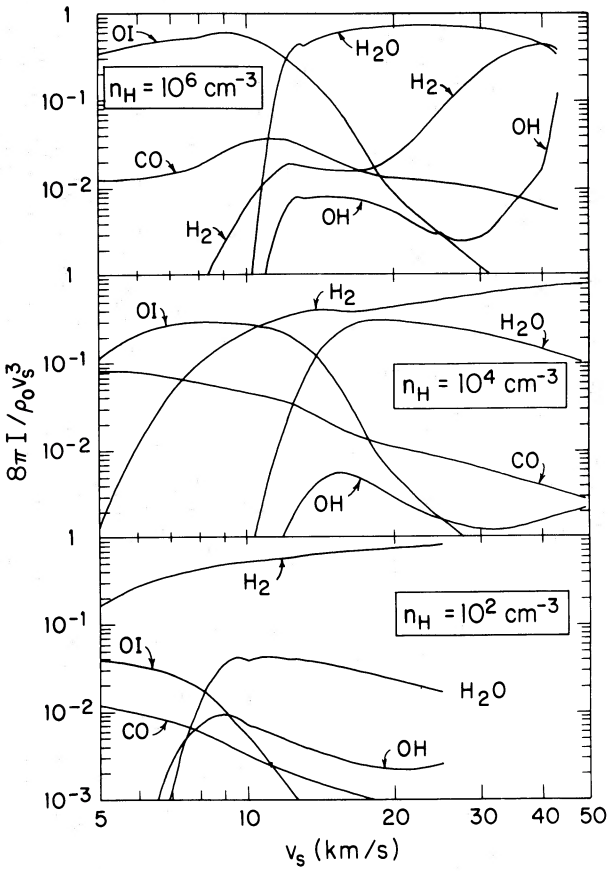

FIG. 4.—The normalized power radiated by the principal coolants, as a function of the shock speed v_s, in molecular gas with preshock $n_H = 10^2$ cm^{-3}, $x_e = 10^{-4}$, and $B_0 = 10$ μG; $n_H = 10^4$ cm^{-3}, $x_e = 10^{-7}$, $B_0 = 100$ μG; and $n_H = 10^6$ cm^{-3}, $x_e = 10^{-8}$, $B_0 = 1.0$ mG.

due to a balance between the increasing heating rate and increasing H_2O abundance. When most of the oxygen has been converted to H_2O, the temperature resumes its rise until the heating rate begins to fall.

c) *Line Emission*

Ground-based infrared spectrometers are able to detect and measure spectral line intensities of about 10^{-3} ergs cm^{-2} s^{-1} sr^{-1} at 12.28 μm (Beck, Lacy, and Geballe 1979), 10^{-4} ergs cm^{-2} s^{-1} sr^{-1} at ~ 3.7 μm (Knacke and Young 1981), and 2×10^{-5} ergs cm^{-2} s^{-1} sr^{-1} at ~ 2.1 μm (Fischer *et al.* 1980). Airborne telescopes can detect [O I] 63 μm line intensities of $\sim 2\times10^{-3}$ ergs cm^{-2} s^{-1} sr^{-1} (Russell *et al.* 1980), and [C I] 609 μm intensities of $\sim 2\times10^{-6}$ ergs cm^{-2} s^{-1} sr^{-1} (Phillips *et al.* 1980). We have computed the intensities of the C I and O I fine structure lines and H_2 vibration-rotation quadrupole lines for our model shock waves.

Line intensities for the diffuse cloud shock models are well below the detection thresholds, and have not been plotted. In Figures 5 and 6 we show the intensities, normal to the shock front, of the C I and O I fine structure lines, together with 10 selected quadrupole lines of H_2, as functions of the shock speed v_s, for shock waves propagating into $n_H = 10^4$ and 10^6 cm^{-3} molecular gas. The line intensities in Figures 5 and 6 are labeled by wavelength (μm). The transitions are listed in Table 5. At low shock speeds the lower rotational levels of H_2 are excited, but at shock speeds in excess of ~ 20 km s^{-1} the $v = 1$ levels of H_2 attain appreciable populations, resulting in the emission of various $v = 1 \rightarrow 0$ lines, in particular the $1 \rightarrow 0$ $S(1)$ line at 2.12 μm.

The $n_H = 10^4$ and 10^6 cm^{-3} shock models suggest that the best emission lines to employ in a search for MHD shock waves in molecular clouds are [O I] 63.1 μm, which is sensitive to shock speeds $\lesssim 10$ km s^{-1}; the H_2 $v = 0 \rightarrow 0$ $S(3)$, $S(5)$, and $S(7)$ lines; and the $v = 1 \rightarrow 0$ $S(1)$ line. The far infrared and millimeter wave rotational lines of CO, OH, and H_2O may also be detectable in many cases; CO line emission from these shocks is examined in detail elsewhere (Draine and Roberge 1983).

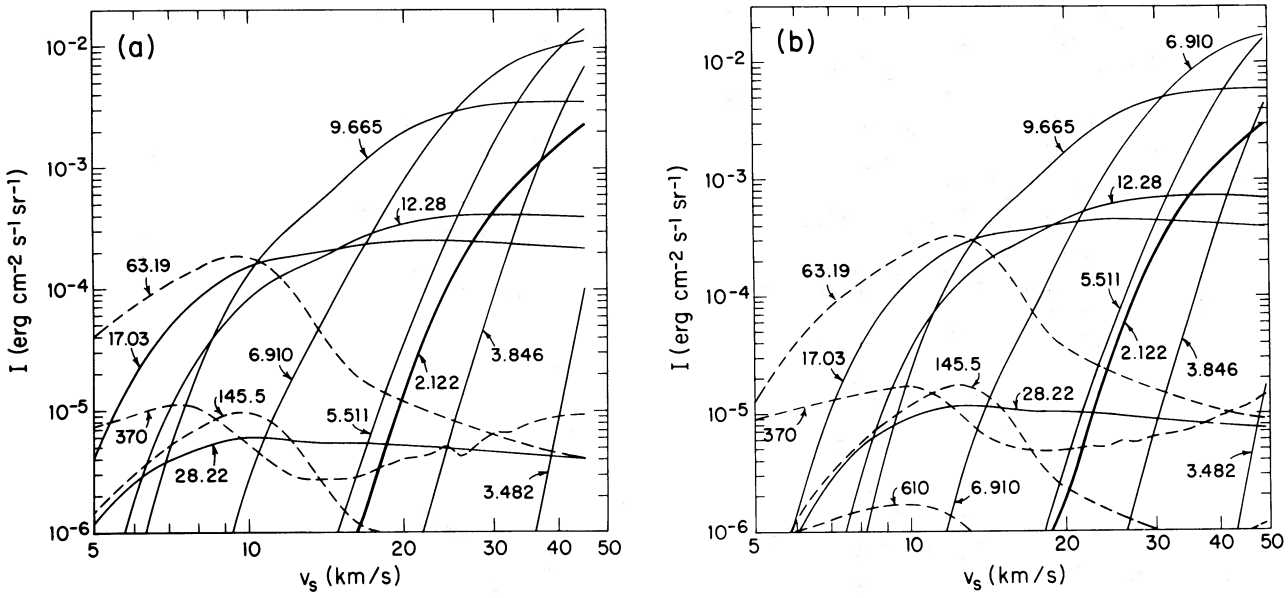

FIG. 5.—Intensities (normal to shock front) for plane-parallel shock waves propagating with shock speed v_s into molecular gas with $n_H = 10^4$ cm^{-3}, $x_e = 10^{-7}$, and (*a*) $B_0 = 50$ μG; (*b*) $B_0 = 100$ μG.

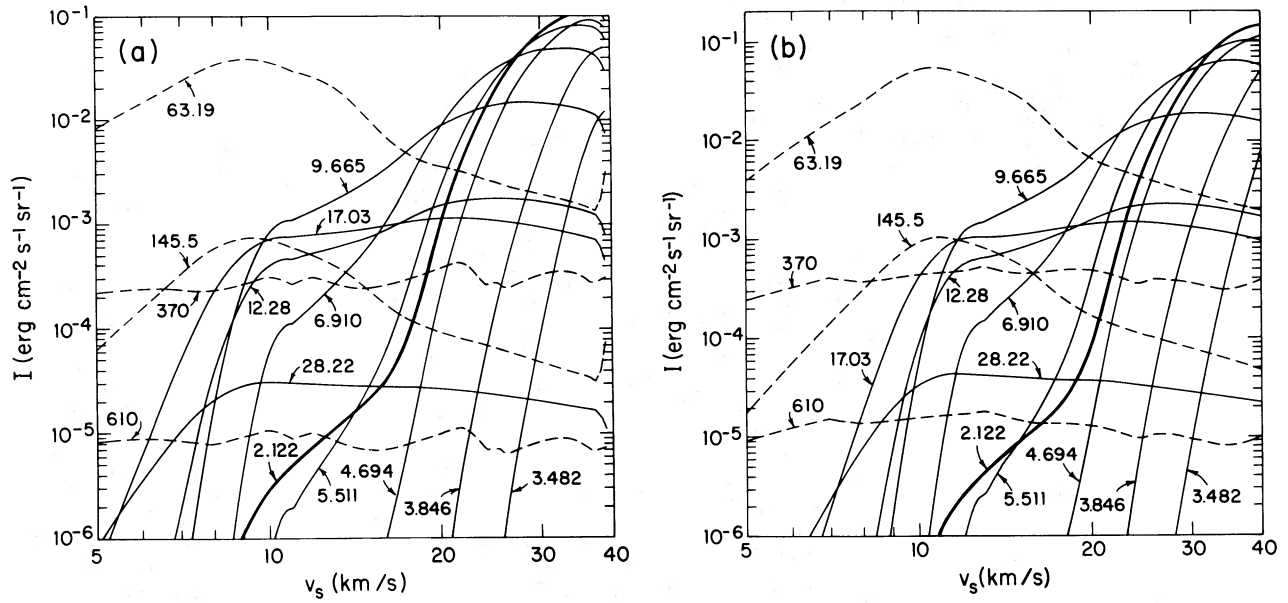

FIG. 6.—Intensities (normal to shock front) for plane-parallel shock waves propagating with shock speed v_s into molecular gas with $n_H = 10^6$ cm^{-3}, $x_e = 10^{-8}$, and (*a*) $B_0 = 0.5$ mG; (*b*) $B_0 = 1$ mG.

The H_2 quadrupole lines remain optically thin in all of the shocks studied here. Radiative transfer effects can, however, affect the intensities of some of the atomic fine structure lines (which were computed assuming the lines to be optically thin) in the $n_H = 10^6$ cm^{-3} models. Specifically, the O I 63.19 μm line develops an optical depth of order unity in the $n_H = 10^6$ cm^{-3} models with $v_s \lesssim 10$ km s^{-1}, so that the O I 63.19 μm intensities in Figures 6*a* and 6*b* may be too large by as much as a factor of ~ 3 for $v_s \lesssim 10$ km s^{-1}. The C I 370, 609 μm emission primarily originates from relatively cool, compressed postshock gas, and these lines develop appreciable optical depths in this postshock region. The intensity of the 609 μm line is accurate to within a factor ~ 2, but the 370 μm line intensities in Figures 6*a* and 6*b*

TABLE 5

SPECTRAL LINES IN FIGURES 5 AND 6

λ(μm)	Transition
609.13[a].....	C I $^3P_1 \rightarrow {}^3P_0$
370.41[a].....	C I $^3P_2 \rightarrow {}^3P_1$
145.53[b]	O I $^3P_0 \rightarrow {}^3P_1$
63.19[b]	O I $^3P_1 \rightarrow {}^3P_2$
28.22	$H_2 v = 0 \rightarrow 0\ S(0)$
17.03	$0 \rightarrow 0\ S(1)$
12.28	$0 \rightarrow 0\ S(2)$
9.665	$0 \rightarrow 0\ S(3)$
6.910	$0 \rightarrow 0\ S(5)$
5.511	$0 \rightarrow 0\ S(7)$
4.694	$0 \rightarrow 0\ S(9)$
3.846	$0 \rightarrow 0\ S(13)$
3.483	$0 \rightarrow 0\ S(17)$
2.122	$v = 1 \rightarrow 0\ S(1)$

[a]Saykally and Evenson 1980.
[b]Moore 1976.

are probably too large, by a factor of up to ~ 10. In addition, the C I 370, 609 μm line intensities computed here are really upper limits, because chemical reactions in the shocked gas which could convert C I into molecular species (e.g., $C + H_2 \rightarrow CH + H$) were neglected, thereby resulting in an upper bound on the C I abundance.

After corrections for differential extinction, observed H_2 quadrupole line intensities can be used to infer ratios of column densities $N(v, J)$ from which an apparent excitation temperature can be obtained:

$$\theta(v_2, J_2; v_1, J_1) \equiv \frac{[E(v_2, J_2) - E(v_1, J_1)]}{k} \left[\ln\left(\frac{g(J_2) N(v_1, J_1)}{g(J_1) N(v_2, J_2)} \right) \right]^{-1}, \tag{65}$$

where $g(J)$ is the degeneracy of level (v, J). Such excitation temperatures are independent of the unknown angle between the line of sight and direction of propagation of the shock, and provide a useful shock diagnostic. In Figures 7, 8, and 9 we present excitation temperatures, as functions of shock speed, for five different preshock conditions. In each figure we show three different rotational excitation temperatures: one which is relevant for the lower rotational levels [(0,11)/(0,3)], one describing the higher rotational levels [(0,17)/(0,11)], and one characterizing the relative rotational populations of the $v = 1$ levels. The rotational excitation temperature of the $v = 2$ level is found to be nearly the same as that for $v = 1$ and is not plotted. These excitation temperatures can be used to compute intensities of H_2 lines not plotted in Figures 5–7; in particular, the intensities of various lines from vibrationally excited states can be readily computed using the plotted intensity of the $v = 1 \rightarrow 0\ S(1)$ line, equation (65), level energies from Waech and Bernstein (1967), and transition probabilities from Turner, Kirby-Docken, and Dalgarno (1977).

For the $n_H = 10^2$ cm^{-3} models, the three rotational temperatures, though (coincidentally) similar to one another, are well below the peak neutral kinetic temperature attained in the shock, primarily because the radiative decay of the $J = 11$ level (and higher levels) is much more rapid than the collisional de-excitation rate at these densities. Similarly, the vibrational levels are far from LTE in these shocks. For preshock $n_H = 10^4$ cm^{-3}, the rotational and vibrational levels continue to be far from LTE, as is evident by the broad range in excitation temperatures at a given shock speed in Figure 8*a* or 8*b*. Only for preshock density $n_H = 10^6$ cm^{-3} do the rotationally and vibrationally excited levels begin to approach a Boltzmann distribution, as is evident from the bunching together of the various excitation temperatures in Figures 9*a* and 9*b*. Even for preshock densities $n_H = 10^6$ cm^{-3}, Figure 9 shows that the vibrational levels deviate significantly from LTE. At low shock speeds $v_s \lesssim 15$ km s^{-1} vibrational excitation of the H_2 is primarily effected by the tenuous but hot electron gas, so that the vibrational excitation temperatures actually exceed the peak neutral kinetic temperatures for low shock speeds in Figures 8 and 9.

Each shock wave contains a broad range of kinetic temperatures, running from the preshock value to the peak value so that even if all levels are in LTE at each point in the shock, the excitation temperatures inferred from the integrated column densities will, in general, differ from one another and from the peak value. Thus in the $n_H = 10^6$ cm^{-3} models for $v_s = 35$ km s^{-1}, $\theta(0,11; 0,3)$ is significantly below $\theta(0,17; 0,11)$ because these shock waves have an extended region with temperatures $T_n \approx 300$ K which are able to appreciably excite the (0,3) level without contributing to the (0,11)

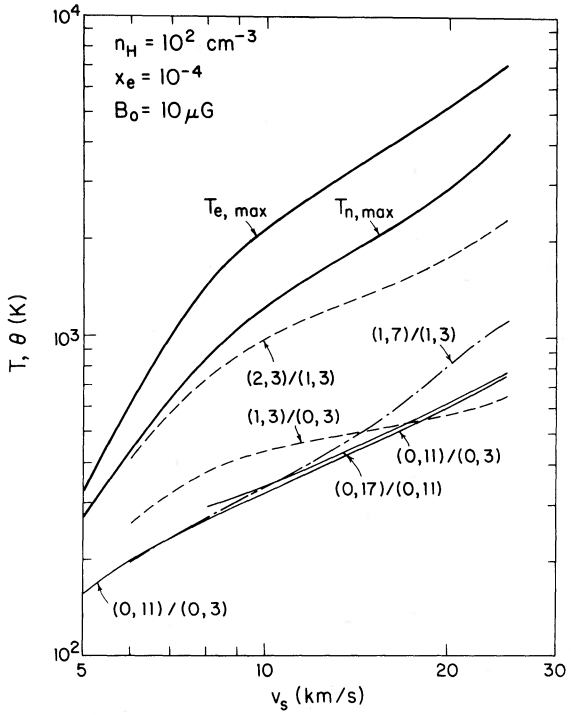

FIG. 7.—Excitation temperatures for various H_2 excited states in shocks of shock speed v_s propagating into $n_H = 10^2$ cm^{-3} diffuse molecular gas with $x_e = 10^{-4}$ and $B_0 = 10\ \mu$G. The "excitation temperatures" are derived from the ratio of column densities; curves are labeled by $(v_2, J_2)/(v_1, J_1)$.

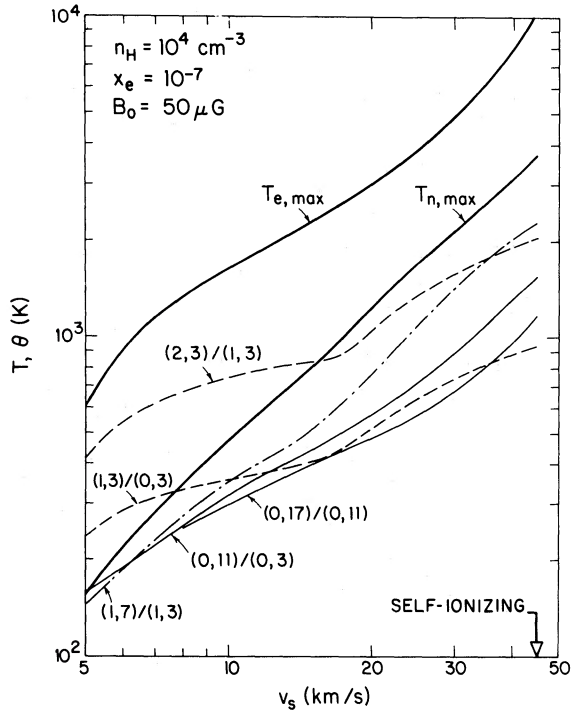

FIG. 8*a*

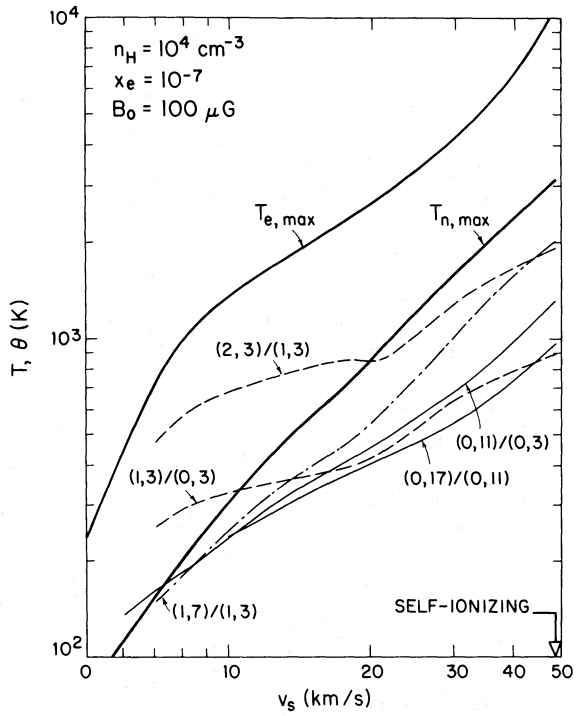

FIG. 8*b*

FIG. 8.—Same as Fig. 7, but for $n_H = 10^4$ cm^{-3} molecular clouds with $x_e = 10^{-7}$ and (*a*) $B_0 = 50\ \mu$G; (*b*) $B_0 = 100\ \mu$G

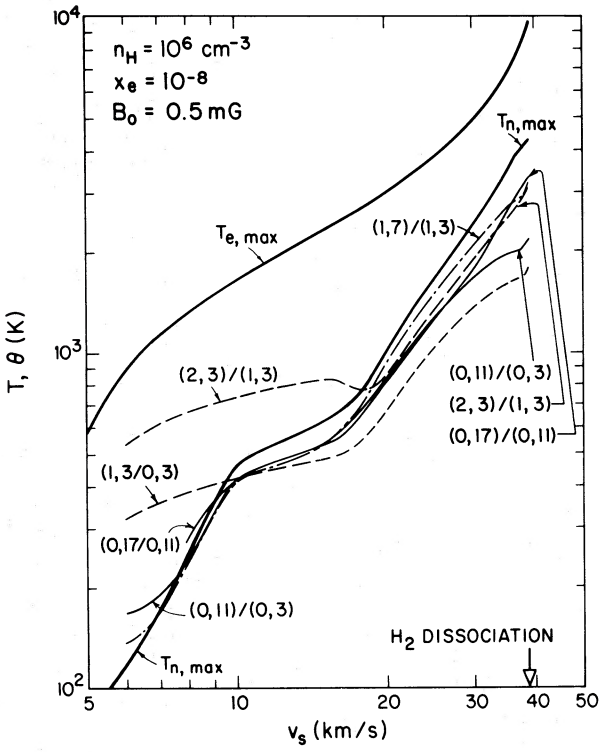

FIG. 9*a*

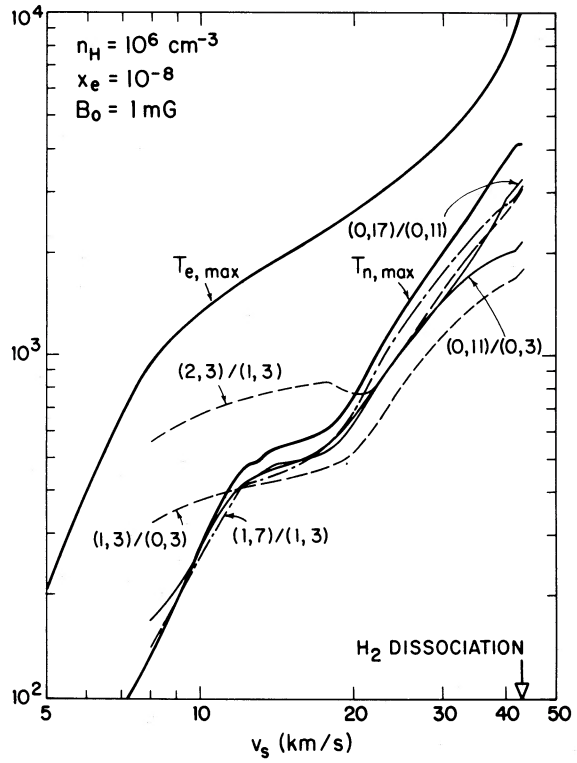

FIG. 9*b*

FIG. 9.—Same as Fig. 8, but for $n_H = 10^6$ cm^{-3} molecular clouds with $x_e = 10^{-8}$ and (*a*) $B_0 = 0.5$ mG; (*b*) $B_0 = 1.0$ mG

column density, and a less extensive region of higher kinetic temperature where (0, 11) and higher energy levels are primarily excited.

d) *Grain Mantle Erosion*

In Figure 10 we plot the fractional volume $[1-(a_f/a_i)^3]$ removed from H_2O ice grains of initial radii $a_i = 0.4$ μm by sputtering in the shock wave. It appears that H_2O ice mantles, and mantles of more volatile ices such as $CH_4/NH_3/H_2O$ mixtures, will be completely returned to the gas phase if the shock speed exceeds about 25 km s^{-1}. This conclusion differs somewhat from that of a previous detailed study (Draine and Salpeter 1979*b*) which employed the same sputtering yields but found $v_s \approx 35$ km s^{-1} to be required for 50% of the volume of a 0.3 μm H_2O ice grain to be removed. Ion-neutral slip was ignored in the earlier work, so that the grain moved relative to the postshock gas only until slowed by gas drag, whereas the magnetic field in the present shock models continues to drive the charged dust grains through the neutral gas throughout the region of ion-neutral slip. Hence the grains suffer a larger number of high-velocity collisions with neutral atoms and molecules than they would in the absence of a magnetic field. Since icy mixtures are less tightly bound than H_2O, any molecules tied up in icy grain mantles will be largely returned to the gas phase in shocks with $v_s \gtrsim 25$ km s^{-1}. Refractory grain cores, however, have binding energies an order of magnitude larger than for H_2O, and will be almost unaffected by sputtering at these shock speeds. *Molecular gas shocked with $v_s \gtrsim 20$ km s^{-1} may be rich in molecules resulting from the sputtering of grain mantles, a consequence which may be relevant to recent observations of "shock-enhanced" chemical abundances* (Dickinson *et al.* 1980; Denoyer and Frerking 1981).

We have neglected the effects of betatron acceleration (Spitzer 1976) on the grain motions. For betatron acceleration to be important, the magnetic field must be compressed in a time short compared to the gas drag damping time τ, but long compared to the gyroperiod; this condition is expressed by the double inequality

$$1 < \left| \frac{dv_i}{dz} \tau \right| < \omega\tau. \tag{66}$$

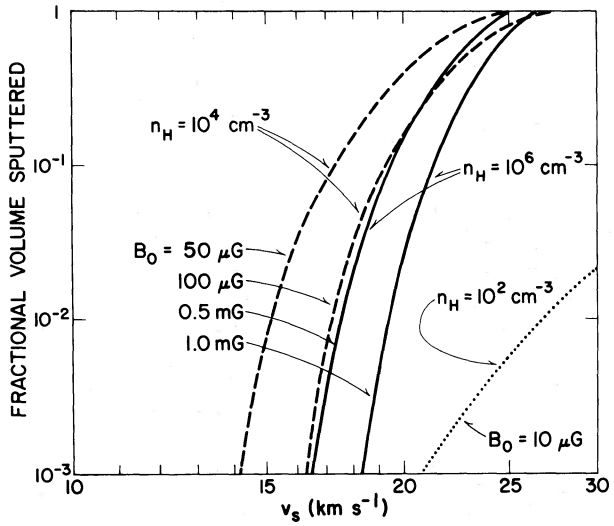

FIG. 10.—Erosion of H_2O ice mantles by sputtering (see text). Curves, labeled by preshock n_H and B_0, show fractional volume sputtered, $[1-(a_f/a_i)^3]$, where $a_i = 0.4$ μm is the initial grain radius, and a_f is the final grain radius.

Each of the $n_H = 10^2$ cm^{-3}, $B_0 = 10$ microgauss shock models has a region in which the double inequality (66) is satisfied, so that betatron acceleration may affect the grain dynamics in these shock waves. For higher preshock density and lower fractional ionizations, however, gas drag damping of the grain motion is strong and (66) is not satisfied. Betatron acceleration appears to be unimportant for $n_H \gtrsim 10^4$ cm^{-3}.

We have neglected the effects of grain-grain collisions in the postshock gas. Shull (1977) estimated that about 4% of the refractory grains are destroyed by grain-grain collisions in $v_s = 20$ km s^{-1} shocks. In the present shock models, with the neutral and charged fluids having different velocities over an appreciable distance, conditions are favorable for grain-grain collisions even if betatron acceleration is not important. Because the grains have a range of sizes, and because they orbit around magnetic field lines, there will be a substantial zone in many of these shock waves where grain-grain collisions may be occurring at an appreciable rate. Grain-grain collisions may be an important grain destruction process in these shock waves, and should be reinvestigated.

e) Uncertainties

The present work has employed a number of simplifications and idealizations. Perhaps foremost has been the assumption that the angle ϑ_B between the preshock magnetic field $\boldsymbol{B}_0$ and the shock velocity vector $\boldsymbol{v}_s$ is 90°. The magnetic field affects the shock structure primarily through its component transverse to the shock. Two shocks with (B_0, ϑ_B) and (B_0', ϑ_B') will be very similar in structure provided $B_0 \sin\vartheta_B = B_0' \sin\vartheta_B'$. Thus, the "weak field" shock models we have computed should provide a good description of shocks propagating at an angle $\vartheta_B = 30°$ relative to a "standard" strength magnetic field. It will be of considerable interest, however, to explicitly compute MHD shock models in which $\vartheta_B < 90°$; this will be undertaken in future work.

The strengths of the magnetic fields present in molecular clouds are uncertain and the existence of the *C*-type shock waves discussed in the present work depends upon the presence of reasonably strong magnetic fields. However, even if the magnetic fields in clouds are an order of magnitude weaker than we have assumed, magnetic precursors will still play a major role in the shock structure. In the $n_H = 10^4$ and 10^6 cm^{-3} cases, we have computed shock models for very weak magnetic fields and find that in many cases the shock waves are still *C*-type even if B_0 is only 10% of our standard value.

The (preshock) fractional ionization in dense molecular clouds is not yet firmly established and is presumably somewhat variable even among clouds of the same density. A modest variation in the preshock fractional ionization will, however, have only a minor effect on the structure of (and emission from) the $n_H = 10^4$ and 10^6 cm^{-3} shock models, since most of the momentum transfer from magnetic field to neutral gas is effected by charged dust grains rather than by the ions. For example, at the hottest point in the shock of Figure 2, approximately 75% of the momentum transfer is due to dust grains, and only 25% is due to ions. Thus the fractional ionization could be changed by a factor of 2 with not more than a 25% change in the peak momentum transfer rate. Similarly, at the hottest point in the shock of Figure 3, 88% of the momentum transfer is due to dust, and only 12% due to ions. Roughly speaking, the

present shock models are only weakly sensitive to changes in the fractional ionization for $x_e \lesssim 2\times10^{-7}$ for $n_{\rm H}=10^4$ cm^{-3}, and $x_e \lesssim 5\times10^{-8}$ for $n_{\rm H}=10^6$ cm^{-3}. These $n_{\rm H}\geqslant 10^4$ cm^{-3} models, in which momentum transfer is dominated by the dust grains, are of course sensitive to the assumed dust characteristics. If the same mass in dust is distributed among more numerous, smaller grains, then the coupling between neutral gas and magnetic field, and consequent heating of the neutral gas, will be enhanced. We have here employed dust parameters which we believe to be appropriate to dense molecular clouds. (In our $n_{\rm H}=10^2$ cm^{-3} calculations, the dust grains are unimportant because of the much larger fractional ionization; conversely, these models *are* sensitive to the assumed fractional ionization.)

It has also been assumed that the velocity distributions of the electrons, ions, and neutral particles could be represented by Maxwellian velocity distributions with different center-of-mass velocities for neutrals and charged particles. This is probably an adequate approximation for processes for which the cross sections do not depend strongly on energy. However, the velocity distribution of the neutral particles will have a nonthermal high velocity tail consisting of those atoms or molecules which have recently undergone collisions with streaming ions or dust grains. The electrons and ions will also have non-Maxwellian velocity distributions. These departures will not affect qualitatively any of the conclusions of the present paper, but these nonthermal velocity distributions merit further study.

As stated in § II, the inertia of the dust grains has been neglected in the present work. Since the dust grain mass density ($\sim 10^{-2}\ \rho_n$) is orders of magnitude larger than the ion density ρ_i in low fractional ionization clouds, it is not obvious that the inertial effects of the dust grains are unimportant. The grains are relatively weakly coupled to the magnetic field in the low-temperature leading edge of the disturbance, so that they have little effect there on the motion of the charged fluid, but this is not the case once the electron temperature has risen above $\sim 10^3$ K and the grains become sufficiently charged that they are more strongly coupled to the magnetic field than to the neutral fluid. A more detailed treatment of the dynamics, with inclusion of grain inertia, will be undertaken in the future.

We have used a simplified treatment of the chemistry of potentially important coolants to show that chemistry can proceed rapidly in the hot shock-heated gas. Further study is required to ascertain whether or not our reaction network omits any reactions which have an important effect on the abundances of the principal atomic and molecular coolants. In particular, reactions such as $OH+CO\rightarrow CO_2+H$ may proceed rapidly in the shock-heated region, possibly affecting the abundance in the shock-heated region of molecules with permanent electric dipole moments, thereby modifying the cooling of the hot molecular gas.

It should be noted that the presence of ion-neutral streaming may play an important role in the chemical reaction network, since the large kinetic energies available in ion-neutral collisions may help drive endothermic reactions, such as the dissociation of H_2 and other molecules (discussed above in § VI*b* and § VII) as well as the formation of molecular ion species in the shocked gas.

Sputtering of grain mantles injects atoms, radicals, and molecules into the gas phase. Our treatment of the gas phase chemistry has neglected this source. As seen in Figure 10, mantle erosion is important for $v_s > 20$ km s^{-1} shock waves, and further studies of shock chemistry should include the effects of grain erosion and destruction.

XI. SUMMARY

The magnetic fields and fractional ionizations thought to be present in molecular clouds are such that the structure of $v_s < 50$ km s^{-1} shock waves may be dramatically different from the conventional one-fluid description of the hydrodynamics. In particular, shock waves in molecular clouds may commonly be *C*-type MHD shock waves, in which the hydrodynamic variables are all continuous and the gas temperature remains well below the one-fluid shock temperature $\sim 3\mu v_s^2/16k$. Our results demonstrate that in dense molecular clouds *C*-type shock waves will be the norm, and *J*-type shocks the exception, unless we have appreciably overestimated the magnetic field strengths in these regions.

We have computed intensities of the rotation-vibration lines of H_2 and of the fine structure lines of O I and C I for various preshock densities and shock speeds. Our results confirm the earlier suggestion (Kwan 1977; Hollenbach and Shull 1977; London, McCray and Chu 1977) that shock waves in dense molecular clouds produce intense H_2 emission, but the minimum speed $v_{\rm dis}$ for H_2 dissociation is found to be considerably greater than the earlier estimate of 24 km s^{-1}: for example $v_{\rm dis}\approx 43$ km s^{-1} for $n_{\rm H}=10^6$ cm^{-3}. The increase in $v_{\rm dis}$ may be relevant to observations of the Orion OMC-1 cloud core, where much of the 2 μm emission apparently originates from H_2 at velocities from 30 to 50 km s^{-1} (Scoville *et al.* 1982; Nadeau, Geballe, and Neugebauer 1982). Recent studies (Draine and Roberge 1982; Chernoff, Hollenbach, and McKee 1982) have shown that shock waves of the kind discussed here are highly successful in accounting for the observed intense emission from H_2, CO, and OH in OMC-1. Collisional excitation in shock-heated gas may also produce the observed H_2 2 μm emission from other molecular clouds, planetary nebulae, and Herbig-Haro objects (cf. Beckwith *et al.* 1980; Fischer, Righini-Cohen, and Simon 1980; Elias 1980; Beckwith and Zuckerman 1981; Persson *et al.* 1981; Bally and Lane 1982).

Chemical reactions may proceed rapidly in the shock-heated molecular gas (cf. Aannestad 1973; Iglesias and Silk 1978; Elitzur and Watson 1980; Hartquist, Oppenheimer, and Dalgarno 1980), producing detectable emission by species other than H_2. Our results show that chemical reactions that produce OH and H_2O play an important role in the thermal structure. At densities $n_H \gtrsim 10^4$ cm^{-3} and shock speeds $v_s \gtrsim 10$ km s^{-1}, H_2O produced in the shock is abundant and is a major coolant.

Even though the betatron effect is generally unimportant, magnetic fields can contribute substantially to grain destruction by driving the charged dust grains through a much larger column density of gas than they would penetrate if acted on only by gas drag. Grain mantle erosion may contribute to "shock-enhanced" abundances of various molecules.

We wish to acknowledge helpful discussions with D. Chernoff, D. J. Hollenbach, W. Langer, G. Melnick, C. F. McKee, J. M. Shull, and L. Spitzer. This work was supported by the National Science Foundation through grants PHY79-19884 and AST9-06373.

REFERENCES

Aannestad, P. 1973, *Ap. J. Suppl.*, **25**, 223.
Bally, J. 1982, *Ap. J.*, **260**, in press.
Bally, J., and Lada, C. J. 1982, preprint.
Bally, J., and Lane, A. P. 1982, *Ap. J.*, **257**, 612.
Beck, S. C., Bloemhof, E. E., Serabyn, E., Townes, C. H., Tokunaga, A. T., Lacy, J. H., and Smith, H. A. 1982, *Ap. J. (Letters)*, **253**, L83.
Beck, S. C., Lacy, J. H., and Geballe, T. R. 1979, *Ap. J. (Letters)*, **234**, L213.
Beckwith, S., Neugebauer, G., Becklin, E. E., Mathews, K., and Persson, S. E. 1980, *A.J.*, **85**, 886.
Beckwith, S., Persson, S. E., Neugebauer, G., and Becklin, E. E. 1978, *Ap. J.*, **223**, 464.
Beckwith, S., and Zuckerman, B. 1981, *Ap. J.*, **255**, 536.
Blais, N. C., and Truhlar, D. G. 1982, *Ap. J. (Letters)*, **258**, L79.
Blevin, H. A., Fletcher, J., and Hunter, S. R. 1978, *Australian J. Phys.*, **31**, 299.
Breshears, W. S., and Bird, P. F. 1973, *Symp. (Int.) Combustion*, **14**, 211.
Carrasco, L., Strom, S. E., and Strom, K. M. 1973, *Ap. J.*, **182**, 95.
Chernoff, D. F., Hollenbach, D. J., and McKee, C. F. 1982, *Ap. J. (Letters)*, **259**, L97.
Chu, S.-I 1979, private communication.
Chung, S., and Lin, C. C. 1978, *Phys. Rev. A*, **17**, 1874.
Cooper, V. G., May, A. D., and Gupta, B. K. 1970, *Canadian J. Phys.*, **48**, 725.
Cravens, T. E., and Dalgarno, A. 1978, *Ap. J.*, **219**, 750.
Crompton, R. W., Gibson, D. K., and McIntosh, A. I. 1969, *Australian J. Phys.*, **22**, 715.
Crutcher, R. M., Troland, T., and Heiles, C. 1981, *Ap. J.*, **249**, 134.
Dalgarno, A., and Roberge, W. G. 1979, *Ap. J. (Letters)*, **233**, L25.
Davis, D. S., Larson, H. P., and Smith, H. A. 1982, *Ap. J.*, **259**, 166.
de Jong, T., Dalgarno, A., and Boland, W. 1980, *Astr. Ap.*, **91**, 68.
Dennison, B. 1977, *Ap. J.*, **215**, 529.
Denoyer, L. K., and Frerking, M. A. 1981, *Ap. J. (Letters)*, **246**, L37.
Dickinson, D. F., Rodriguez Kuiper, E. N., Dinger, A. S. C., and Kuiper, T. B. H. 1980, *Ap. J. (Letters)*, **237**, L43.
Dickman, R. L. 1978, *Ap. J. Suppl.*, **37**, 407.
Dove, J. E., and Teitelbaum, H. 1974, *Chem. Phys.*, **6**, 431.
Draine, B. T. 1980, *Ap. J.*, **241**, 1021 (see also *Ap. J.*, **246**, 1045 [1981]).
_____. 1981, *Ap. J.*, **245**, 880.
Draine, B. T., and Roberge, W. G. 1982, *Ap. J. (Letters)*, **259**, L91.
_____. 1983, in preparation.
Draine, B. T., and Salpeter, E. E. 1979*a*, *Ap. J.*, **231**, 77.
_____. 1979*b*, *Ap. J.* **231**, 438.
Drawin, H. W. 1968, *Z. Phys.*, **211**, 404.
_____. 1969, *Z. Phys.*, **225**, 483.
Dyck, H. M., and Beichman, C. A. 1974, *Ap. J.*, **194**, 57.
Ehrhardt, H., Langhans, L., Linder, F., and Taylor, H. S. 1968, *Phys. Rev.*, **173**, 222.
Elias, J. H. 1980, *Ap. J.*, **241**, 728.
Elitzur, M., and de Jong, T. 1978, *Astr. Ap.*, **78**, 323.
Elitzur, M., and Watson, W. D. 1978, *Astr. Ap.*, **70**, 443.
Elitzur, M., and Watson, W. D. 1980, *Ap. J.*, **236**, 172.
Elmegreen, B. G. 1979, *Ap. J.*, **222**, 729.
Fischer, J., Righini-Cohen, G., and Simon, M. 1980, *Ap. J. (Letters)*, **238**, L155.
Fischer, J., Righini-Cohen, G., Simon, M., Joyce, R. R., and Simon, T. 1980, *Ap. J. (Letters)*, **240**, L95.
Fliflet, A. W., and McKoy, V. 1980, *Phys. Rev. A*, **21**, 1863.
Frerking, M. A., and Langer, W. D. 1982, *Ap. J.*, **256**, 523.
Frerking, M. A., Langer, W. D., and Wilson, R. W. 1982, *Ap. J.*, **262**, 590.
Gautier, T. N., Fink, U., Treffers, R. R., and Larson, H. P. 1976, *Ap. J. (Letters)*, **207**, L129.
Gear, C. W. 1971, *Numerical Initial Value Problems in Ordinary Differential Equations* (Englewood Cliffs: Prentice Hall).
Genzel, R., Reid, M. J., Moran, J. M., and Downes, D. 1981, *Ap. J.*, **244**, 884.
Gerjuoy, E., and Stein, S. 1955, *Phys. Rev.*, **97**, 1671.
Goldsmith, P. F., *et al.* 1981, *Ap. J. (Letters)*, **243**, L79.
Graedel, T. E., Langer, W. D., and Frerking, M. A. 1982, *Ap. J. Suppl.*, **48**, 321.
Green, S., Ramaswamy, R., and Rabitz, H. 1978, *Ap. J. Suppl.*, **36**, 483.
Green, S., and Truhlar, D. G. 1979, *Ap. J. (Letters)*, **231**, L101.
Guélin, M., Langer, W. D., Snell, R. L., and Wootten, H. A. 1977, *Ap. J. (Letters)*, **217**, L165.
Guélin, M., Langer, W. D., and Wilson, R. W. 1982, *Astr. Ap.*, **107**, 107.
Hartquist, T. W. Oppenheimer, M., and Dalgarno, A. 1980, *Ap. J.*, **236**, 182.
Hayden, H. C., and Utterback, N. G. 1964, *Phys. Rev. A.*, **135**, 1575.
Heiles, C. 1976, *Ann. Rev. Astr. Ap.*, **14**, 1.
Hollenbach, D., and McKee, C. F. 1979, *Ap. J. Suppl.*, **41**, 555.
_____. 1980, *Ap. J. (Letters)*, **241**, L47.
_____. 1981, private communication.
Hollenbach, D., and Shull, J. M. 1977, *Ap. J.*, **216**, 419.
Iglesias, E. R., and Silk, J. P. 1978, *Ap. J.*, **226**, 851.
Johnson, P. E., Rieke, G. H., Lebofsky, M. J., and Kemp, J. C. 1981, *Ap. J.*, **245**, 871.
Knacke, R. F., and Young, E. T. 1980, *Ap. J. (Letters)*, **242**, L183.
_____. 1981, *Ap. J. (Letters)*, **249**, L65.
Knapp, G. R., Phillips, T. G., Huggins, P. J., and Redman, R. O. 1981, *Ap. J.*, **250**, 175.
Kuiper, T. B. H., Rodriguez Kuiper, E. N., and Zuckerman, B. 1978, *Ap. J.*, **219**, 129.
Kwan, J. 1977, *Ap. J.*, **216**, 713.
Kwan, J., and Scoville, N. Z. 1976, *Ap. J. (Letters)*, **210**, L39.
Lada, C. J., and Harvey, P. M. 1981, *Ap. J.*, **245**, 58.
Launay, J. M., and Roueff, E. 1977, *Astr. Ap.*, **56**, 289.
Linder, F., and Schmidt, H. 1971, *Z. Naturf.*, **26a**, 1603.
London, R., McCray, R., and Chu, S.-I. 1977, *Ap. J.*, **217**, 442.
Loren, R. B., Erickson, N., Snell, R. L., Mundy, L., and Davis, J. H. 1981, *Ap. J. (Letters)*, **244**, L107.
Loren, R. B., Mundy, L., and Erickson, N. R. 1981, *Ap. J.*, **250**, 573.
Lotz, W. 1967, *Ap. J. Suppl.*, **14**, 207.

McKee, C. F., Storey, J. W. V., Watson, D. M., and Green, S. 1982, *Ap. J.*, **259**, 647.
Meyer, J. P. 1979, in *Les Elements et Leurs Isotopes dans L'Univers*, 22nd Liège Internat. Astrophysics Symposium (University of Liège Press), p. 153.
Monchick, L., and Schaefer, J. 1980, *J. Chem. Phys.*, **73**, 6153.
Moore, C. E. 1976, *Selected Tables of Atomic Spectra*: O I (Washington: NSRDS–NBS 3, § 7).
Mullan, D. J. 1971, *M.N.R.A.S.*, **153**, 145.
Nadeau, D., and Geballe, T. R. 1979, *Ap. J.* (*Letters*), **230**, L169.
Nadeau, D., Geballe, T. R., and Neugebauer, G. 1982, *Ap. J.*, **253**, 154.
Nussbaumer, H., and Rusca, C. 1979, *Astr. Ap.*, **72**, 129.
Ogden, P. M., Roesler, F. L., Larson, H. P., Smith, H. A., Reynolds, R. J., and Sehert, F. 1979, *Ap. J.* (*Letters*), **233**, L21.
Péquignot, D., and Aldrovandi, S. M. V. 1976, *Astr. Ap.*, **50**, 141.
Persson, S. E., Geballe, T. R., Simon, T., Lonsdale, C. J., and Baas, F. 1981, *Ap. J.* (*Letters*), **251**, L85.
Phelps, A. V. 1979, in *Electron-Molecule Scattering*, ed. S. C. Brown (New York: Wiley), p. 81.
Phillips, T. G., and Huggins, P. J. 1981, *Ap. J.*, **251**, 533.
Phillips, T. G., Huggins, P. J., Kuiper, T. B. H., and Miller, R. E. 1980, *Ap. J.* (*Letters*), **238**, L103.
Prasad, S. S., and Huntress, W. T. 1980, *Ap. J. Suppl.*, **43**, 1.
Procaccia, I., and Levine, R. D. 1975, *J. Chem. Phys.*, **63**, 4261.
Purcell, E. M. 1979, *Ap. J.*, **231**, 404.
Reid, J., and McKellar, A. R. W. 1978, *Phys. Rev. A*, **18**, 224.
Roberge, W. G., and Dalgarno, A. 1982, *Ap. J.*, **255**, 176.
Rodriguez, L. F., Carral, P., Ho, P. T. P., and Moran, J. M. 1982, *Ap. J.*, **260**, 635.
Russell, R. W., Melnick, G., Gull, G. E., and Harwit, M. 1980, *Ap. J.* (*Letters*), **240**, L99.
Savage, B. D., and Mathis, J. S. 1979, *Ann. Rev. Astr. Ap.*, **17**, 73.
Saykally, R. J., and Evenson, K. M. 1980, *Ap. J.* (*Letters*), **238**, L107.
Scoville, N. Z., Hall, D. N. B., Kleinmann, S. G., and Ridgway, S. T. 1982, *Ap. J.*, **253**, 136.
Shull, J. M. 1977, *Ap. J.*, **215**, 805.
Simon, M., Righini-Cohen, G., Joyce, R. R., and Simon, T. 1979, *Ap. J.* (*Letters*), **230**, L175.
Snell, R. L., Loren, R. B., and Plambeck, R. L. 1980, *Ap. J.* (*Letters*), **239**, L17.
Solomon, P. M., Huguenin, G. R., and Scoville, N. Z. 1981, *Ap. J.* (*Letters*), **245**, L19.
Spitzer, L. 1976, *Comments Ap.*, **6**, 177.
Srivastava, S. K., and Jensen, S. 1977, *J. Phys. B*, **10**, 3341.
Stacey, G. J., Kurtz, N. T., Smyers, S. D., Harwit, M., Rusell, R. W., and Melnick, G. 1982, *Ap. J.* (*Letters*), **257**, L37.
Storey, J. W. V., Watson, D. M., Townes, C. H., Heller, E. E., and Hansen, W. L. 1981, *Ap. J.*, **247**, 136.
Tarr, S. M., and Rabitz, H. 1978, *J. Chem. Phys.*, **68**, 647.
Turner, B. E., and Zuckerman, B. 1978, *Ap. J.* (*Letters*), **225**, L75.
Turner, J., Kirby-Docken, K., and Dalgarno, A. 1977, *Ap. J. Suppl.*, **35**, 281.
Umebayashi, T., and Nakano, T. 1980, *Pub. Astr. Soc. Japan*, **32**, 4.
Van Zyl, B., Le, T. Q., and Amme, R. C. 1981, *J. Chem. Phys.*, **74**, 314.
Van Zyl, B., and Utterback, N. G. 1969, *Sixth Int. Conf. Phys. Electron. Atom. Collisions* (Cambridge: MIT), p. 393.
Verschuur, G. L. 1979, *Fund. Cosmic Phys.*, **5**, 113.
van Vliet, A. H. F., de Graauw, Th., Lee, T. J., Lidholm, S., and Stadt, H. V. D. 1981, *Astr. Ap.*, **101**, L1.
Waech, T. G., and Bernstein, R. B. 1967, *J. Chem. Phys.*, **46**, 4905.
Watson, D. M., Storey, J. W. V., Townes, C. H., Heller, E. E., and Hansen, W. L. 1980, *Ap. J.* (*Letters*), **239**, L129.
Watson, W. D., Snyder, L. E., and Hollis, J. M. 1978, *Ap. J.* (*Letters*), **222**, L145.
Weatherland, C. A. 1980, *Phys. Rev. A*, **22**, 2519.
Wiese, W. L., Smith, M. W., and Glennon, B. M. 1966, *Atomic Transition Probabilities*, Vol. **1** (NSRDS–NBS 4; Washington: Government Printing Office).
Williams, J. F., and Willis, B. A. 1974, *J. Phys. B*, **7**, L61.
Wootten, A., Snell, R., and Glassgold, A. E. 1979, *Ap. J.*, **234**, 876.
Zuckerman, B., Kuiper. T. B. H., and Rodriguez Kuiper, E. N. 1976, *Ap. J.* (*Letters*), **209**, L13.

B. T. Draine and W. G. Roberge: Institute for Advanced Study, Princeton NJ 08540

A. Dalgarno: Center for Astrophysics, 60 Garden St., Cambridge MA 02138